

1 **Examination of varying mixed-phase stratocumulus clouds in terms of their**  
2 **properties, ice processes and aerosol-cloud interactions between polar and**  
3 **midlatitude cases: An attempt to propose a microphysical factor to explain the**  
4 **variation**

5

6 Seoung Soo Lee<sup>1,2,3</sup>, Chang-Hoon Jung<sup>4</sup>, Jinho Choi<sup>5</sup>, Young Jun Yoon<sup>6</sup>, Junshik Um<sup>5,7</sup>,  
7 Youtong Zheng<sup>8</sup>, Jianping Guo<sup>9</sup>, Manguttathil. G. Manoj<sup>10</sup>, Sang-Keun Song<sup>11</sup>

8

9 <sup>1</sup>Science and Technology Corporation, Hampton, Virginia

10 <sup>2</sup>Earth System Science Interdisciplinary Center, University of Maryland, College Park,  
11 Maryland, USA

12 <sup>3</sup>Research Center for Climate Sciences, Pusan National University, Busan, Republic of  
13 Korea

14 <sup>4</sup>Department of Health Management, Kyungin Women's University, Incheon, Republic of  
15 Korea

16 <sup>5</sup>Department of Atmospheric Sciences, Pusan National University, Busan, Republic of  
17 Korea

18 <sup>6</sup>Korea Polar Research Institute, Incheon, Republic of Korea

19 <sup>7</sup>Institute of Environmental Studies, Pusan National University, Busan, Republic of Korea

20 <sup>8</sup>Department of Earth and Atmospheric Sciences, University of Houston, Houston, Texas,  
21 USA

22 <sup>9</sup>State Key Laboratory of Severe Weather, Chinese Academy of Meteorological Sciences,  
23 Beijing 100081, China

24 <sup>10</sup>Advanced Centre for Atmospheric Radar Research, Cochin University of Science and  
25 Technology, Kerala, India

26 <sup>11</sup>Department of Earth and Marine Sciences, Jeju National University, Jeju, Republic of  
27 Korea

28

29

30

31

32

33

34

35

36

37

38

39

40

41

42

43

44

45

46

47

48 Corresponding author: Seoung Soo Lee, Chang-Hoon Jung and Sang-Keun Song

49 Office: (303) 497-6615

50 Cell: (609) 375-6685

51 Fax: (303) 497-5318

52 E-mail: [cumulss@gmail.com](mailto:cumulss@gmail.com), [slee1247@umd.edu](mailto:slee1247@umd.edu)

## 53 Abstract

54

55 This study examines the ratio of ice crystal number concentration (ICNC) to cloud droplet  
56 number concentration (CDNC), which is ICNC/CDNC, in mixed-phase stratocumulus  
57 clouds. This examination is performed using a large-eddy simulation (LES) framework and  
58 one of efforts toward a more general understanding of mechanisms controlling cloud  
59 development, aerosol-cloud interactions and impacts of ice processes on them in mixed-  
60 phase stratocumulus clouds. For the examination, this study compares a case of polar  
61 mixed-phase stratocumulus clouds to that of midlatitude mixed-phase stratocumulus  
62 clouds with weak precipitation. It is found that ICNC/CDNC plays a critical role in making  
63 differences in cloud development with respect to the relative proportion of liquid and ice  
64 mass between the cases by affecting in-cloud latent-heat processes. Note that this  
65 proportion has an important implication for cloud radiative properties and thus climate. It  
66 is also found that ICNC/CDNC plays a critical role in making differences in interactions  
67 between clouds and aerosols and impacts of ice processes on clouds and their interactions  
68 with aerosols between the cases by affecting in-cloud latent-heat processes. Findings of  
69 this study suggest that ICNC/CDNC can be a simplified general factor that contributes to  
70 a more general understanding and parameterizations of mixed-phase clouds, their  
71 interactions with aerosols and roles of ice processes in them.

72

73

74

75

76

77

78

79

80

81

82

83

**Deleted:** and thus, to the development of more general parameterizations of those clouds, interactions and roles

## 86 1. Introduction

87

88 Stratiform clouds (e.g., stratus and stratocumulus clouds) have significant impacts on  
 89 climate (Warren et al. 1986; Stephens and Greenwald 1991; Hartmann et al. 1992; Hahn  
 90 and Warren 2007; Wood, 2012; Dione et al., 2019; Zheng et al., 2021). Since  
 91 industrialization, aerosol concentrations have increased and this has had impacts on  
 92 stratiform clouds and climate (Twomey, 1974; Albrecht, 1989; Ackerman et al., 2004).  
 93 However, our level of understanding of these clouds and impacts has been low and this has  
 94 caused the highest uncertainty in the prediction of future climate (Ramaswamy et al., 2001;  
 95 Forster et al., 2007; Knippertz et al., 2011; Hannak et al., 2017). Stratiform clouds can be  
 96 classified into warm and mixed-phase clouds. Mixed-phase stratiform clouds involve ice  
 97 processes and frequently form in midlatitude and polar regions. When mixed-phase  
 98 stratiform clouds are associated with convective clouds, they can form even in the tropical  
 99 region. Most previous studies have focused on warm clouds and their interactions with  
 100 aerosols, whereas the mixed-phase stratiform clouds and their interactions with aerosols  
 101 are poorly understood mainly due to the more complex ice processes. Hence, mixed-phase  
 102 stratiform clouds and their interactions with aerosols account for the uncertainty more than  
 103 warm clouds and their interactions with aerosols (Ramaswamy et al., 2001; Forster et al.,  
 104 2007; Wood, 2012; IPCC, 2021; Li et al., 2022).

Deleted: .

Formatted: Font: Not Italic

Deleted: This is because radiative properties of liquid particles are substantially different from those of ice particles.

Formatted: Font: Not Italic

Deleted: 2022

105 The relative proportion of liquid mass, which can be represented by liquid-water  
 106 content (LWC) or liquid-water path (LWP), and ice mass, which can be represented by ice-  
 107 water content (IWC) or ice-water path (IWP), in mixed-phase stratiform clouds plays a  
 108 critical role in cloud radiative properties and thus their climate feedbacks (Tsushima et  
 109 al., 2006; Choi et al., 2010 and 2014; Gottelman et al., 2012; Zhang et al., 2019). The  
 110 relative proportion is defined to be IWC (IWP) over LWC (LWP) or IWC/LWC  
 111 (IWP/LWP) in this study. Motivated by this and the above-mentioned uncertainty, this  
 112 study aims to improve our understanding of mixed-phase stratiform clouds and their  
 113 interactions with aerosols with the emphasis on ice processes and IWC/LWC (or  
 114 IWP/LWP).

115 Lee et al. (2021) have investigated mixed-phase stratocumulus clouds in a midlatitude  
 116 region and found that microphysical latent-heat processes are more important in the

121 development of mixed-phase stratiform clouds and their interactions with aerosols than  
 122 entrainment and sedimentation processes. Lee et al. (2021) have found that a microphysical  
 123 factor, the ratio of ice crystal number concentration (ICNC) to cloud droplet number  
 124 concentration (CDNC) or ICNC/CDNC, play an important role in latent processes, the  
 125 development of mixed-phase stratiform clouds and their interactions with aerosols. In  
 126 particular, Lee et al. (2021) have found that IWC/LWC or IWP/LWP is strongly affected  
 127 by ICNC/CDNC. This is because deposition and condensation of water vapor occur on the  
 128 surface of ice crystals and droplets, respectively. Thus, ice crystals and droplets act as  
 129 sources of deposition and condensation, respectively. Then, ice crystals and droplets act  
 130 as sources of IWC (or IWP) and LWC (or LWP), respectively. More ice crystals and  
 131 droplets provide the greater integrated surface area of ice crystals and droplets and induce  
 132 more deposition and condensation, respectively, for a given environmental condition (Lee  
 133 et al., 2009; Khain et al., 2012; Fan et al., 2018; Chua and Ming, 2020; Lee et al., 2021).  
 134 The higher ICNC/CDNC means more ice crystals or sources of deposition per a droplet as  
 135 a source of condensation in a given group of ice crystals and droplets. Thus, the higher  
 136 ICNC/CDNC enables more deposition per unit condensation to occur, which can raise  
 137 IWC/LWC or IWP/LWP.

138 Mixed-phase stratocumulus clouds in different regions are known to have different  
 139 IWC/LWC or IWP/LWP and aerosol-cloud interactions (e.g., Choi et al., 2010 and 2014;  
 140 Zhang et al., 2019). Lots of factors such as environmental conditions, which can be  
 141 represented by variables such as temperature, humidity and wind shear, and macrophysical  
 142 factors one of which is the relative locations of ice-crystal and droplet layers, can explain  
 143 those differences. Choi et al. (2010 and 2014) and Zhang et al. (2019) have shown that as  
 144 temperature lowers, IWC/LWC or IWP/LWP tends to increase and indicated that  
 145 temperature is a primary environmental condition to explain the differences in IWC/LWC  
 146 among different regions or clouds. However, Choi et al. (2010 and 2014) and Zhang et al.  
 147 (2019) have not discussed process-level mechanisms that govern the role of temperature in  
 148 those differences.

149 It is important to establish a general principle that explains the differences in  
 150 LWC/LWC and aerosol-cloud interactions among regions, since the general principle is  
 151 useful in the development of a more general or comprehensive parameterization of

Deleted: 2022

Deleted: 2022

Deleted: (

Deleted: )

Deleted: s

Deleted: (

Deleted: )

Deleted: (

Deleted: )

Deleted: (

Deleted: )

Deleted: (

Deleted: )

Deleted: and then

Deleted: (

Deleted: .

Deleted: ( droplets)

Deleted: (

Deleted: )

Deleted: (

Deleted: )

Deleted: 2022

Deleted: Note that deposition and condensation are processes through which water vapor is removed, hence ice crystals and droplets are sinks of water vapor when deposition and condensation occur. However, when it comes to deposition and condensation themselves as microphysical processes, ice crystals (droplets) can be considered the sources of deposition and condensation.

Deleted:

179 stratocumulus clouds and their interactions with aerosols for climate models. This  
 180 contributes to the better prediction of future climate, considering that the absence of the  
 181 comprehensive parameterization has been considered one of the biggest obstacles to the  
 182 better prediction (Ramaswamy et al., 2001; Foster et al., 2007; Stevens and Feingold, 2009).

183 As a way of contributing to the establishment of the general principle, this study  
 184 attempts to take ICNC/CDNC as a general factor, which can constitute the general principle,  
 185 to explain the differences in IWC/LWC (or IWP/LWP) and aerosol-cloud interactions  
 186 among clouds. This study also attempts to elucidate how ice processes differentiate mixed-  
 187 phase stratiform clouds from warm clouds in terms of cloud development and its  
 188 interactions with aerosols, and how this differentiation varies among cases of mixed-phase  
 189 stratiform clouds with different ICNC/CDNC values. This attempt is valuable, considering  
 190 that in general, the establishment of the general principle for stratocumulus clouds and their  
 191 interactions with aerosols has been progressed much less than that for other types of clouds  
 192 such as convective clouds and their interactions with aerosols. The attempt is valuable, also  
 193 considering that our level of understanding of how ice processes differentiate mixed-phase  
 194 stratiform clouds and their interactions with aerosols from much-studied warm clouds and  
 195 their interactions with aerosols has been low. Here, we want to emphasize that this study  
 196 does not aim to gain a fully established general principle, but aims to test the factor that  
 197 can be useful to move ahead on our path to a more complete general principle. Hence, this  
 198 study should be regarded a steppingstone to the established principle, and should not be  
 199 considered a perfect study that get us the fully established principle. Taking into account  
 200 the fact that even attempts to provide general factors for the general principle have been  
 201 rare, the fulfilment of the aim is likely to provide us with valuable preliminary information  
 202 that streamlines the development of a more established general principle. ▼

203 For the attempt, this study investigates a case of mixed-phase stratiform clouds in the  
 204 polar region. Via the investigation, this study aims to identify process-level mechanisms  
 205 that control the development of those clouds and their interactions with aerosols, and the  
 206 impact of ice processes on the development and interactions using a large-eddy simulation  
 207 (LES) framework. Then, this study compares the mechanisms in the case of polar clouds  
 208 to those in a case of midlatitude clouds which have been examined by Lee et al. (2021).  
 209 This comparison is based on Choi et al. (2010 and 2014) and Zhang et al. (2019) which

Deleted: .

Deleted:

Deleted:

Deleted: 2022

214 have shown that temperature is an important factor which explains the differences in  
 215 IWC/LWC among regions or clouds. Due to significant differences in latitudes, noticeable  
 216 differences in the temperature of air are between the polar and midlatitude cases. Hence,  
 217 through this comparison, this study looks at the role of temperature in those differences in  
 218 IWC/LWC and associated aerosol-cloud interactions. More importantly than that, as a way  
 219 of identifying process-level mechanisms that control the role of temperature, this study  
 220 tests how ICNC/CDNC as the general factor is linked to the role of temperature, using the  
 221 LES framework. Through this test, this study also identifies process-level mechanisms that  
 222 control how ICNC/CDNC affects roles of ice processes in the differentiation between  
 223 mixed-phase stratiform and warm clouds in terms of cloud development and its interactions  
 224 with aerosols, and causes the variation of the differentiation between the cases of mixed-  
 225 phase stratiform clouds.

Deleted:

## 227 2. Case, model and simulations

228

### 229 2.1 LES model

230

231 LES simulations are performed by using the Advanced Research Weather Research and  
 232 Forecasting (ARW) model. A bin scheme, which is detailed in Khain et al. (2000) and  
 233 Khain et al. (2011), is adopted by the ARW for the simulation of microphysics. Size  
 234 distribution functions for each class of hydrometeors, which are classified into water drops,  
 235 ice crystals (plate, columnar and branch types), snow aggregates, graupel and hail, are  
 236 represented with 33 mass doubling bins, i.e., the mass of a particle  $m_k$  in the  $k$ th bin is  
 237 determined as  $m_k = 2m_{k-1}$ . Each of hydrometeors has its own terminal velocity that varies  
 238 with the hydrometeor mass and the sedimentation of hydrometeors is simulated using their  
 239 terminal velocity.

Deleted: , which are classified into water drops, ice crystals (plate, columnar and branch types), snow aggregates, graupel and hail,

Deleted: and aerosols acting as cloud condensation nuclei (CCN) and ice-nucleating particles (INP)

Moved (insertion) [1]

Deleted:

240 Size distribution functions for aerosols, which act as cloud condensation nuclei  
 241 (CCN) and ice-nucleating particles (INP), adopt the same mass doubling bins as for  
 242 hydrometeors. The evolution of aerosol size distribution and associated aerosol  
 243 concentrations at each grid point is controlled by aerosol sinks and sources such as aerosol  
 244 advection, turbulent mixing, activation and aerosol regeneration via the evaporation of

Moved up [1]: Each of hydrometeors has its own terminal velocity that varies with the hydrometeor mass and the sedimentation of hydrometeors is simulated using their terminal velocity. T

Deleted: and

256 droplets and the sublimation of ice crystals. Aerosol regeneration follows the method  
257 similar to that as described in Xue et al. (2010). It is assumed that aerosols do not fall down  
258 by themselves and move around by airflow that is composed of horizontal flow, updrafts,  
259 downdrafts and turbulent motions. When aerosols move with airflow, it is assumed that  
260 they move with the same velocity as airflow. Taking activation as an example of the  
261 evolution of aerosol size distribution, the bins of the aerosol spectra that correspond to  
262 activated particles are emptied. Activated aerosol particles are included in hydrometeors  
263 and move to different classes and sizes of hydrometeors through collision-coalescence. In  
264 case hydrometeors with aerosol particles precipitate to the surface, those particles are  
265 removed from the atmosphere.

Formatted: Font: (Asian) Times New Roman, (Asian) Korean

266 The large energetic turbulent eddies are directly resolved by the LES framework, and  
267 the effects of the smaller subgrid-scale turbulent motions on the resolved flow are  
268 parameterized based on a most widely used method that Smagorinsky (1963) and Lilly  
269 (1967) proposed. In this method, the mixing time scale is defined to be the norm of the  
270 strain rate tensor (Bartosiewicz and Duponcheel, 2018). A cloud-droplet nucleation  
271 parameterization based on Köhler theory represents cloud-droplet nucleation. Arbitrary  
272 aerosol mixing states and aerosol size distributions can be fed to this parameterization. To  
273 represent heterogeneous ice-crystal nucleation, the parameterizations by Lohmann and  
274 Diehl (2006) and Möhler et al. (2006) are used. In these parameterizations, contact,  
275 immersion, condensation-freezing, and deposition nucleation paths are all considered by  
276 taking into account the size distribution of INP, temperature and supersaturation.  
277 Homogeneous aerosol (or haze particle) and droplet freezing is  
278 also considered following the theory developed by Koop et al. (2000).

Deleted: the

279 The bin microphysics scheme is coupled to the Rapid Radiation Transfer Model  
280 (RRTM; Mlawer et al., 1997). The effective sizes of hydrometeors, which are calculated  
281 in the bin scheme, are fed into the RRTM as a way of considering effects of the effective  
282 sizes on radiation. The surface process and resultant surface heat fluxes are simulated by  
283 the interactive Noah land surface model (Chen and Dudhia, 2001).

284

## 285 **2.2 Case and simulations**

286



### 2.2.1 Case and standard simulations

288  
289  
290 In the Svalbard area, Norway, a system of mixed-phase stratocumulus clouds existed over  
291 the horizontal domain marked by a red rectangle in Figure 1 and a period between 02:00  
292 and 10:00 local solar time (LST) on March 29<sup>th</sup>, 2017. These clouds are observed by the  
293 Cloudnet ground observation that has been established to provide a systematic evaluation  
294 of clouds in forecast and climate models. The Cloudnet observation aims to establish a  
295 number of ground-based remote sensing sites, which would all be equipped with a specific  
296 array of instrumentation, using active sensors such as lidar and Dopplerized mm-wave  
297 radar, in order to provide vertical profiles of the main cloud variables (e.g., LWP and IWP),  
298 at high spatial and temporal resolution (Hogan et al., 2006). The Cloudnet observation  
299 provides data of important cloud variables such as LWP and IWP to the public and this  
300 study utilize these data.

301 On average, the bottom and top of the observed clouds, which are measured by radar  
302 and lidar in the Cloudnet observation, are at ~400 m and ~3 km in altitude, respectively.  
303 The simulation of the observed system or case, i.e., the control run, is performed three-  
304 dimensionally over the red rectangle and the period between 02:00 and 10:00 LST on  
305 March 29<sup>th</sup>, 2017. The horizontal domain adopts a 100-m resolution for the control run. The  
306 length of the domain in the horizontal directions is 50 km. The length of the domain in the  
307 vertical direction is ~5 km and the resolution for the vertical domain gets coarsened with  
308 height from ~5 m just above the surface to ~150 m at the model top as detailed in the  
309 supplement. Reanalysis data, which are produced by Met Office Unified Model (Brown et  
310 al., 2012) every 6 hours on a  $0.11^\circ \times 0.11^\circ$  grid, provide potential temperature, specific  
311 humidity, and wind as initial and boundary conditions, which represent synoptic-scale  
312 environment, for the control run. The control run employs an open lateral boundary  
313 condition. Figure 2a shows the vertical distribution of the domain-averaged potential  
314 temperature and humidity in those reanalysis data at the first time step. A neutral, mixed  
315 layer is between the surface and 1 km in altitude as an initial condition (Figure 2a). Figure  
316 2b shows the time evolution of the domain-averaged large-scale subsidence or downdraft  
317 in the reanalysis data and at the model top. This large-scale subsidence is imposed on the  
318 control run as a part of background wind fields and interacts with updrafts and downdrafts

Deleted: ~

Deleted: local solar time (LST)

Deleted:

Deleted: ground radar and lidar and these radar and lidar are a part of the Cloudnet ground observation that is deployed at a location in the red rectangle

Deleted: . The Cloudnet ground observation is composed of a suite of instruments such as lidar, radar and radiometer and described in Hogan et al. (2006).

Deleted: se

Deleted: , according to observation by those radar and lidar

Deleted:

Deleted: 20

Deleted:

Deleted: 0

334 generated by relatively small-scale processes including those associated with clouds. The  
 335 large-scale subsidence gradually reduces with time (Figure 2b). Figure 2c shows the time  
 336 evolution of the domain-averaged surface temperature in the reanalysis data. This evolution  
 337 of the surface temperature is mostly controlled by the sea surface temperature considering  
 338 that most portion of the red-rectangle domain is accounted for by the ocean (Figure 1). Due  
 339 to the sunrise, the surface temperature starts to increase more rapidly around 08:00 LST  
 340 (Figure 2c).

341 The properties of cloud condensation nuclei (CCN) such as the number concentration,  
 342 size distribution and composition are measured in the domain (Tunved et al., 2013; Jung et  
 343 al., 2018). The measurement of the CCN concentration has been carried out at the Zeppelin  
 344 research station in the domain, using the commercial droplet measurement technologies  
 345 CCN counter with one column (CCNC-100), managed by the Korea Polar Research  
 346 Institute, since year 2007. The CCNC-100 measures the CCN concentration at  
 347 supersaturations of 0.2, 0.4, 0.6, 0.8 and 1% (Jung et al., 2018). The aerosol number size  
 348 distribution is observed using a closed-loop differential mobility particle sizer (DMPS).  
 349 The DMPS charges aerosol particles and exposing them into an electric field, which causes  
 350 them to experience a force proportional to their electrical mobility, resulting in their  
 351 classification according to size (Tunved et al., 2013). Aerosol composition is measured  
 352 using aerosol mass spectrometry (AMS). The AMS measures the composition by  
 353 vaporizing and ionizing aerosol particles.

354 The measurement indicates that on average, aerosol particles are an internal mixture  
 355 of 70 % ammonium sulfate and 30 % organic compound. This mixture is assumed to  
 356 represent aerosol chemical composition over the whole domain and simulation period for  
 357 this study. The observed and averaged concentration of aerosols acting as CCN is  $\sim 200$   
 358  $\text{cm}^{-3}$  over the simulation period between 02:00 and 10:00 LST on March 29<sup>th</sup>, 2017. Note  
 359 that the average of a variable with respect to time in the rest of this paper is performed over  
 360 this period between 02:00 and 10:00 LST, unless otherwise stated.  $200 \text{ cm}^{-3}$  as the averaged  
 361 concentration of aerosols acting as CCN is interpolated into all of grid points immediately  
 362 above the surface at the first time step.

363 This study does not take into account aerosol effects on radiation before aerosol is  
 364 activated, since no significant amount of radiation absorbers is found in the mixture. Based

Deleted: .

Deleted: (SST)

Deleted: Between ~06:00 LST around when

Deleted:

Deleted: s and ~08:00 LST

Deleted: s from -2.2 to -1.6 °C,

Deleted: and after that, it does not show significant increase or decrease ...

Formatted: Font: (Asian) Malgun Gothic

Formatted: Font: Not Italic

Deleted: Based on this,

Deleted: an

Formatted: Font: Italic, Font color: Auto

375 on observation, the size distribution of aerosols acting as CCN is assumed to be a tri-modal  
 376 log-normal distribution (Figure 3). The shape of distribution, which is a tri-modal log-  
 377 normal distribution, as shown in Figure 3 is applied to the size distribution of aerosols  
 378 acting as CCN in all parts of the domain during the whole simulation period. The assumed  
 379 shape in Figure 3 is obtained by performing the average on the observed size distribution  
 380 parameters (i.e., modal radius and standard deviation of each of nuclei, accumulation and  
 381 coarse modes, and the partition of aerosol number among those modes) over the simulation  
 382 period. Note that although these parameters or the shape of aerosol size distribution does  
 383 not vary, associated aerosol concentrations vary over the simulation domain and period via  
 384 processes as described in Section 2.1. This study takes an assumption that the interpolated  
 385 CCN concentrations do not vary with height in a layer between the surface and the  
 386 planetary boundary layer (PBL) top around 1 km in altitude at the first time step, following  
 387 the previous studies such as Gras (1991), Jaenicke (1993) and Seinfeld and Pandis (1998).  
 388 However, above the PBL top, they are assumed to decrease exponentially with height at  
 389 the first time step, based on those previous studies, although the shape of size distribution  
 390 and composition do not change with height. It is assumed that the properties of INP and  
 391 CCN are not different except for concentrations. The concentration of aerosols acting as  
 392 CCN is assumed to be 100 times higher than that acting as INP over grid points at the first  
 393 time step based on a general difference in concentrations between CCN and INP  
 394 (Pruppacher and Klett, 1978). Hence, the concentration of aerosols acting as INP at the  
 395 first time step is  $2 \text{ cm}^{-3}$  in the control run. This assumed concentration of aerosols acting  
 396 as INP is higher than usual (Seinfeld and Pandis, 1998). However, Hartmann et al. (2021)  
 397 observed the INP concentration that was at the same order of magnitude as assumed here  
 398 in the Svalbard area when strong dust events occur, meaning that the assumed INP  
 399 concentration is not that unrealistic.

400 To examine effects of aerosols on mixed-phase clouds, the control run is repeated by  
 401 increasing the concentration of aerosols by a factor of 10. In the repeated (~~control~~) run, the  
 402 initial concentrations of aerosols acting as CCN and INP at grid points immediately above  
 403 the surface are 2000 (200) and  $20 \text{ (2) cm}^{-3}$ , respectively. Reflecting these concentrations in  
 404 the simulation name, the control run is referred to as “the 200\_2 run” and the repeated run  
 405 is referred to as “the 2000\_20 run”. To isolate effects of aerosols acting as CCN (~~INP~~), on

Deleted:

Deleted: .

Deleted: higher than

Formatted: Font: (Asian) Times New Roman

Deleted: (

Deleted: )

Deleted: (

Deleted: )

413 mixed-phase clouds, the control run is repeated again by increasing the concentration of  
 414 aerosols acting as CCN (INP) only but not INP (CCN) by a factor of 10. In this repeated  
 415 run with the increase in the concentration of aerosols acting as CCN (INP), the initial  
 416 concentrations of aerosols acting as CCN and INP at grid points immediately above the  
 417 surface are 2000 (200) and 2 (20)  $\text{cm}^{-3}$ , respectively. Reflecting this, the repeated run is  
 418 referred to as “the 2000\_2 (200\_20) run”.

419

### 420 2.2.2 Additional simulations

421

422 To isolate impacts of ice processes on the adopted case and its interactions with aerosols,  
 423 the 200\_2 and 2000\_2 runs are repeated by removing ice processes. These repeated runs  
 424 are referred to as the 200\_0 and 2000\_0 runs. In the 200\_0 and 2000\_0 runs, all  
 425 hydrometeors (i.e., ice crystals, snow, graupel, and hail), phase transitions (e.g., deposition  
 426 and sublimation) and aerosols (i.e., INP) which are associated with ice processes are  
 427 removed. Hence, in these runs, only droplets (i.e., cloud liquid), raindrops, associated phase  
 428 transitions (e.g., condensation and evaporation) and aerosols acting as CCN are present,  
 429 regardless of temperature. Stated differently, these noise runs simulate the warm-cloud  
 430 counterpart of the selected mixed-phase cloud system. Via comparisons between a pair of  
 431 the 200\_2 and 2000\_2 runs and a pair of the 200\_0 and 2000\_0 runs, the role of ice  
 432 processes in the differentiation between mixed-phase and warm clouds is to be identified.  
 433 Along with this identification, the role of the interplay between ice crystals and droplets in  
 434 the development of the selected mixed-phase cloud system and its interactions with  
 435 aerosols is to be isolated.

436 As detailed in Sections 3.1.4 and 3.2.2 below, the test of ICNC/CDNC as a general  
 437 factor requires more simulations to see impacts of ICNCavg/CDCNavg on clouds and their  
 438 interactions with aerosols. Here, ICNCavg and CDCNavg represent the average ICNC and  
 439 CDNC over grid points and time steps with non-zero ICNC and CDNC, respectively.  
 440 ICNCavg/CDCNavg represents overall ICNC/CDNC over the domain and simulation  
 441 period. To respond to this requirement, the 200\_0.07, 2000\_0.07 and 200\_0.7 runs are  
 442 performed and their details are given in Sections 3.1.4 and 3.2.2. In addition, all the  
 443 simulations above are repeated by turning off radiative processes and Section 3.3 provides

Deleted: F

Deleted: 200\_2\_noise

Deleted: 2000\_2\_noise

Deleted: 200\_2\_noise

Deleted: 2000\_2\_noise

Deleted: 200\_2\_noise

Deleted: 2000\_2\_noise

Deleted: 2

Deleted: (

Deleted: )

Deleted: s

Deleted: (

Deleted: )

Deleted: (

Deleted: )

Deleted: .

Deleted: 200\_2\_fac10

Deleted: 200\_2\_fac10\_CCN10

Deleted: ,

Deleted: 200\_2\_fac10\_INP10

Deleted: 2

465 the details of these repeated simulations. These repeated runs are the 200\_2\_norad,  
 466 2000\_20\_norad, 2000\_2\_norad, 200\_20\_norad, ~~200\_0~~ norad, ~~2000\_0~~ norad,  
 467 ~~200\_0.07~~ norad, ~~2000\_0.07~~ norad and ~~200\_0.7~~ norad runs. Moreover, based on the  
 468 argument in Section 4.2, the 4000\_45, 13\_0.1, ~~4000\_1.8~~ and ~~12\_0.0035~~ runs are performed  
 469 and details of these runs are provided in Section 4.2. Some of the simulations are  
 470 summarized in Table 1 for better clarification with a brief description of their configuration.

**Deleted:** 200\_2\_noise  
**Deleted:** 2000\_2\_noise  
**Deleted:** 200\_2\_fac10  
**Deleted:** 200\_2\_fac10\_CCN10  
**Deleted:** 200\_2\_fac10\_INP10  
**Deleted:** 4000\_1.8\_fac10  
**Deleted:** 12\_0.0035\_fac10  
**Deleted:**  
**Deleted:** The summary of simulations in this study is given in Table 1.

### 472 3. Results

473

#### 474 3.1 The 200\_2 run vs. the ~~200\_0~~ run

475

##### 476 3.1.1 Model validation

477

478 This study adopts the Cloudnet ground observation to evaluate the 200\_2 run. Observed  
 479 LWP is provided by radiometer in the Cloudnet observation. The retrieval of IWP is  
 480 performed by using radar reflectivity and lidar backscatter in the Cloudnet observation as  
 481 described in Donovan et al. (2001), Donovan and Lammeren (2001), Donovan (2003) and  
 482 Tinel et al. (2005). In the retrieval, the lidar signal and radar reflectivity profiles are  
 483 combined and inverted using a combined lidar/radar equation as a function of the light  
 484 extinction coefficient and radar reflectivity. The combined equation is detailed in Donovan  
 485 and Lammeren (2001). Simulated LWP and IWP, as shown in Figure 4 and Table 2, are  
 486 compared to the observed LWP and retrieved IWP, respectively. The average LWP over  
 487 all time steps and grid columns for the period between 02:00 and 10:00 LST on March 29<sup>th</sup>,  
 488 2017 is 1.23  $\text{g m}^{-2}$  in the 200\_2 run and 1.12  $\text{g m}^{-2}$  in Cloudnet observation. The average  
 489 IWP over all time steps and grid columns over the period is 31.94  $\text{g m}^{-2}$  in the 200\_2 run  
 490 and 29.10  $\text{g m}^{-2}$  in the retrieval. Cloud-bottom height, which is averaged over grid columns  
 491 and time steps with non-zero cloud-bottom height over the period, is 420 and 440 m in the  
 492 200\_2 run and Cloudnet observation, respectively. Cloud-top height, which is averaged  
 493 over grid columns and time steps with non-zero cloud-top height over the period, is 3.5 and  
 494 3.3 km in the 200\_2 run and Cloudnet observation, respectively. Each of LWP, cloud-  
 495 bottom and -top heights shows an ~10% difference between the 200\_2 run and observation.

**Deleted:** 200\_2\_noise

**Formatted:** Outline numbered + Level: 3 + Numbering Style: 1, 2, 3, ... + Start at: 1 + Alignment: Left + Aligned at: 0.75" + Indent at: 1.25"  
**Formatted:** Font: (Default) Batang, (Asian) Batang  
**Formatted:** Indent: Left: 1.25"  
**Deleted:**

**Deleted:** As mentioned above, observed cloud-bottom and -top heights are obtained from radar and lidar measurements.

**Deleted:**  
**Formatted:** Superscript  
**Deleted:**

512 IWP also shows an ~10% difference between the 200\_2 run and the retrieval. Thus, the  
 513 200\_2 run is considered performed reasonably well for these variables.

514 To provide additional information of cloud development, Figure 5 shows the time  
 515 evolution of the simulated and observed cloud-top and bottom heights, simulated and  
 516 retrieved IWP and simulated and observed LWP together with the evolution of the  
 517 simulated surface sensible and latent-heat fluxes; the simulated evolutions in Figure 5 are  
 518 from the 200\_2 run. This is based on the fact that the cloud-top and bottom heights, IWP  
 519 and LWP are considered a good indicative of cloud development and the surface fluxes are  
 520 considered important parameters controlling the overall development of clouds. The cloud-  
 521 top height increases between 02:00 and ~05:00 LST and after ~05:00 LST, it reduces  
 522 gradually. The cloud-bottom height decreases between 02:00 and ~05:00 LST and after  
 523 ~05:00 LST, it does not change much. IWP and LWP show an overall increase between  
 524 02:00 and ~05:30 LST to reach its peak around 05:30 LST and then an overall decrease.  
 525 The surface fluxes reduce with time, although the reduction rate of the fluxes starts to  
 526 decrease around 08:00 LST in association with the rapid increase in the surface temperature  
 527 which starts around 08:00 LST as shown in Figure 2c.

528 The time- and domain-averaged IWP and IWC are ~one order of magnitude greater than  
 529 LWP and LWC, respectively, in the 200\_2 run (Figure 4 and Table 2). For the sake of  
 530 simplicity, the averaged IWC over the averaged LWC is denoted by  $IWC/LWC$ , and the  
 531 averaged IWP over the averaged LWP is by  $IWP/LWP$ , henceforth.  $IWC/LWC$  and  
 532  $IWP/LWP$  are 26.28 and 25.96, respectively, in the 200\_2 run. Since IWP and LWP are  
 533 vertically integrated IWC and LWC over the vertical domain, respectively, the qualitative  
 534 nature of differences between IWC and LWC is not much different from that between IWP  
 535 and LWP. Hence, mentioning both a pair of IWC and LWC and that of IWP and LWP is  
 536 considered redundant, and mentioning either a pair of IWC and LWC or that of IWP and  
 537 LWP enhances the readability. Henceforth, IWC and LWC are chosen to be mentioned in  
 538 text, although all of IWC, LWC, IWP and LWP are displayed in Tables 2 and 3.

539 Choi et al. (2014) and Zhang et al. (2019) have obtained the supercooled cloud fraction  
 540 (SCF), which is basically the ratio of LWC to the sum of LWC and IWC and denoted by  
 541  $LWC/(LWC+IWC)$ , using satellite- and ground-observed data collected over the period of  
 542 ~5 years and ~1 year, respectively. Choi et al. (2014) have shown that SCF is as low as

Deleted:

Deleted: or supplementary

Deleted:

Deleted: is shown

Deleted: simulated

Deleted: in Supplementary Figure 1

Deleted: .

Deleted: is

Deleted: Simulated evolutions in Supplementary Figure 1 are from the 200\_2 run.

Deleted:

Deleted: between ~06:00 and

Deleted: ~

Deleted: (

Deleted: )

Deleted: is

Deleted: (

Deleted: )

Deleted: (IWP)

Deleted: (LWP)

Deleted: (IWP)

Deleted: (LWP)

565 ~0.01 for the temperature range between -16 and -33 °C. Zhang et al. (2019) have also  
 566 shown that SCF is as low as ~0.03 for the same temperature range, although the occurrence  
 567 of SCF of ~0.03 or lower is rare. Note that the average air temperature immediately below  
 568 the cloud base and above the cloud top over the simulation period is -16 and -33 °C,  
 569 respectively, in the 200\_2 run, and SCF in the 200\_2 run is 0.04. Hence, based on Choi et  
 570 al. (2014) and Zhang et al. (2019), we believe that SCF in the 200\_2 run is observable and  
 571 thus not that unrealistic, although it may not occur frequently.

### 572 **3.1.2 Microphysical processes, sedimentation and entrainment**

573  
 574  
 575 To understand process-level mechanisms that control the results, microphysical processes  
 576 are analyzed. As indicated by Ovchinnikov et al. (2011), in clouds with weak precipitation,  
 577 a high-degree correlation is found between IWC and deposition or between LWC and  
 578 condensation, considering that deposition and condensation are sources of IWC and LWC,  
 579 respectively. In the 200\_2 run, the average surface precipitation rate over the simulation  
 580 period is ~0.0020 mm hr<sup>-1</sup>, which can be considered weak. Hence, in this case,  
 581 condensation and deposition are considered proxies for LWC and IWC, respectively. Based  
 582 on this, to gain a process-level understanding of microphysical processes that control the  
 583 simulated LWC and IWC, condensation and deposition are analyzed.

584 As seen in Figure 6 and Table 2, the average deposition rate is ~one order of magnitude  
 585 greater than condensation rate in the 200\_2 run, leading to much greater IWC than LWC  
 586 in the 200\_2 run. This is in contrast to the situation in the case of mixed-phase  
 587 stratocumulus clouds, which were located in a midlatitude region, in Lee et al. (2021). In  
 588 that case, the average IWC and LWC are at the same order of magnitude. For the sake of  
 589 brevity, the case in Lee et al. (2021) is referred to as “the midlatitude case”, while the case  
 590 of mixed-phase clouds, which is adopted by this study, in the Svalbard area is referred to  
 591 “the polar case”, henceforth. In the midlatitude case, IWC/LWC is 1.55, which is ~ one  
 592 order of magnitude smaller than that in the polar case.

593 Warm clouds in the 200\_0 run shows that the time- and domain-averaged condensation  
 594 rate that is lower than the time- and the domain-averaged sum of condensation and  
 595 deposition rates in the 200\_2 run (Figure 6 and Table 2). This leads to a situation where

Formatted: Font: (Asian) Times New Roman, Bold

Formatted: Body Text 3, Left, Automatically adjust right indent when grid is defined, Outline numbered + Level: 3 + Numbering Style: 1, 2, 3, ... + Start at: 1 + Alignment: Left + Aligned at: 0.75" + Indent at: 1.25", Adjust space between Latin and Asian text, Adjust space between Asian text and numbers

Deleted:

Deleted: I

Deleted: L

Deleted: I

Deleted: L

Deleted: 5

Deleted: 2022

Deleted: is

Deleted: is

Deleted: 2022

Deleted: 200\_2\_noise

Deleted: 5



608 warm clouds in the 200\_0 run shows the time- and domain-averaged LWC that is lower  
 609 than the time- and domain-averaged water content (WC), which is the sum of IWC and  
 610 LWC, in mixed-phase clouds in the 200\_2 run (Figure 4 and Table 2). This is despite the  
 611 fact that LWC in the 200\_0 run is higher than LWC in the 200\_2 run (Figure 4 and Table  
 612 2); WC represents the total cloud mass in mixed-phase clouds, while LWC alone represents  
 613 the total cloud mass in warm clouds.

614 It should be noted that the average rate of sedimentation of droplets over the cloud  
 615 base and simulation period reduces from the 200\_0 run to the 200\_2 run (Table 2). This is  
 616 mainly due to the decrease in LWC from the 200\_0 run to the 200\_2 run. The average rate  
 617 of sedimentation of ice crystals over the cloud base and simulation period increases from  
 618 the 200\_0 run to the 200\_2 run, since sedimentation of ice crystals is absent in the 200\_0  
 619 run (Table 2). The average entrainment rate over the cloud top and simulation period  
 620 increases from the 200\_0 run to the 200\_2 run (Table 2). Here, entrainment rate is defined  
 621 to be the difference between the rate of increase in cloud-top height and the large-scale  
 622 subsidence, following Moeng et al. (1999), Jiang et al. (2002), Stevens et al. (2003a and  
 623 2003b) and Ackerman et al. (2004). Entrainment tends to reduce the total cloud mass more  
 624 in the 200\_2 run than in the 200\_0 run. Thus, entrainment should be opted out when it  
 625 comes to mechanisms leading to the increase in the total cloud mass from the 200\_0 run to  
 626 the 200\_2 run. Here, the vertical integration of each of condensation and deposition rates  
 627 is obtained over each cloudy column in the domain for each of the runs. For the sake of the  
 628 brevity, this vertical integrations of condensation and deposition rates are referred to as the  
 629 integrated condensation and deposition rates, respectively. Then, each of the integrated  
 630 condensation and deposition rates is averaged over cloudy columns and the simulation  
 631 period. It is found that the average rates of the droplet and ice-crystal sedimentation over  
 632 the cloud base and simulation period are ~four orders of magnitude smaller than the  
 633 average integrated condensation and deposition rates, respectively, in the 200\_2 run (Table  
 634 2). It is also found that the average rate of the droplet sedimentation over the cloud base  
 635 and simulation period is ~five orders of magnitude smaller than that in the average  
 636 integrated condensation rate in the 200\_0 run (Table 2). Changes in the average rates of  
 637 the droplet and ice-crystal sedimentation over the cloud base and simulation period are  
 638 ~four to five orders of magnitude smaller than those in the average integrated condensation

Deleted: 200\_2\_noise

Deleted: 200\_2\_noise

Deleted: 200\_2\_noise

Deleted: 200\_2\_noise

Deleted: 200\_2\_noise

Deleted: 200\_2\_noise

Deleted: 200\_2\_noise

Deleted: Hence, the droplet sedimentation tends to increase the total cloud mass in the 200\_2 run, and the ice-crystal sedimentation and entrainment tend to reduce the total cloud mass in the 200\_2 run, as compared to that in the 200\_2\_noise run. This means that the droplet sedimentation contributes to increase in the total cloud mass from the 200\_2\_noise run to the 200\_2 run, while entrainment and the ice-crystal sedimentation counter the increase. Thus, entrainment and the ice-crystal sedimentation should be opted out when it comes to mechanisms leading to the increase in the total cloud mass.

Deleted:

Deleted: (

Deleted: )

Deleted: is

Deleted: (

Deleted: )

Deleted: the change in

Deleted: droplet

Deleted: from the 200\_2\_noise run to the 200\_2 run is

Deleted: five to six

Deleted: that in



666 and deposition rates between the 200\_2 and 200\_0 runs (Table 2). Thus, condensation and  
 667 deposition, but not the droplet and ice-crystal sedimentation, are main factors controlling  
 668 cloud mass, which is represented by LWC and IWC, and the total cloud mass in the 200\_2  
 669 and 200\_0 runs, and the variation of cloud mass and the total cloud mass between the runs  
 670 as are in the midlatitude case and its warm-cloud counterpart.

671

672

### 673 3.1.3 Hypothesis

674

675 We hypothesized that ICNC/CDNC can be an important factor that determines above-  
 676 described differences between the polar and midlatitude cases. Note that both in the polar  
 677 and midlatitude cases, pockets of ice particles and those of liquid particles are mixed  
 678 together instead of being separated from each other as seen in Figure 4 and Lee et al. (2021).

679 Remember that ice crystals are more as sources of deposition per a droplet when  
 680 ICNC/CDNC is higher. Thus, when ICNC/CDNC is higher and  $q_v > q_{sw}$ , it is more likely  
 681 that more portion of water vapor is deposited onto ice crystals by stealing water vapor,  
 682 which is supposed to be condensed onto droplets, from droplets in an air parcel. Here,  $q_v$   
 683 and  $q_{sw}$  represent water-vapor pressure and water-vapor saturation pressure for liquid  
 684 water or droplets, respectively. When ICNC/CDNC is higher and  $q_{si} < q_v < q_{sw}$ , more ice  
 685 crystals can absorb water vapor, including that which is produced by droplet evaporation,  
 686 per a droplet; here,  $q_{si}$  represents water-vapor saturation pressure for ice water or ice  
 687 crystals. Thus, with higher ICNC/CDNC, it is more likely that more portion of water vapor  
 688 is deposited onto ice crystals in an air parcel as shown in Lee et al. (2021). Figure 7 shows  
 689 the time series of the averaged supersaturation over grid points where deposition occurs in  
 690 the presence of both droplets and ice crystals in the 200\_2 run. Figure 7 indicates that on  
 691 average, supersaturation occurs for both droplets and ice crystals over those grid points.  
 692 Hence, on average, the above-described situation of  $q_v > q_{sw}$  is applicable to deposition  
 693 when droplets and ice crystals coexist in the 200\_2 run.

694 ICNC<sub>avg</sub>/CDNC<sub>avg</sub> is 0.22 in the control run (i.e., the 200\_2 run) for the polar case  
 695 and 0.019 in the control run for the midlatitude case which is described in Lee et al. (2021).  
 696 Henceforth, the control run for the midlatitude case is referred to as the control-midlatitude

**Deleted:** , the average integrated deposition rate, and the sum of the average integrated condensation and deposition rate (Table 2). Thus, condensation and deposition, but not the droplet sedimentation, are main factors controlling differences in cloud mass, which is represented by LWC and IWC, and in the total cloud mass between the 200\_2 and 200\_2\_noise runs as are between the midlatitude case and its warm-cloud counterpart.

**Deleted:** ¶

**Deleted:** .

**Deleted:** that

**Deleted:** 2022

**Deleted:** 2022

710 run. ICNCavg/CDNCavg is ~one order of magnitude higher for the polar case than for the  
 711 midlatitude case. This is despite the fact that the ratio of the initial number concentration  
 712 of aerosols acting as INP to that of acting as CCN is identical between the 200\_2 and  
 713 control-midlatitude runs. In addition, identical model, model setup such as vertical  
 714 resolutions, and source of reanalysis data are used between the 200\_2 and control-  
 715 midlatitude runs, although there are differences in environmental conditions (e.g.,  
 716 temperature), cloud macrophysical variables such as cloud-top height and horizontal  
 717 resolutions between the runs. Here, while taking these similarities and differences into  
 718 account, we hypothesize that the significant differences in ICNCavg/CDNCavg between  
 719 runs are mainly due to the fact that ice nucleation strongly depends on air temperature  
 720 (Prappacher and Klett, 1978). When supercooling is stronger, in general, more ice crystals  
 721 are nucleated for a given group of aerosols acting as INP. The average air temperature  
 722 immediately below the cloud base over the simulation period is -16 °C in the 200\_2 run  
 723 and -5 °C in the control-midlatitude run. The average air temperature immediately above  
 724 the cloud top is -33 °C in the 200\_2 run and -15 °C in the control-midlatitude run. Hence,  
 725 supercooling is greater and this contributes to the higher ICNCavg/CDNCavg in the polar  
 726 case than in the midlatitude case. The higher ICNCavg/CDNCavg is likely to induce more  
 727 portion of water vapor to be deposited onto ice crystals in the polar case than in the  
 728 midlatitude case. It is hypothesized that this in turn enables IWC/LWC in the 200\_2 run to  
 729 be one order of magnitude greater than that in the control-midlatitude run or in the  
 730 midlatitude case. Much higher IWC than LWC, which results in a much higher IWC/LWC  
 731 in the polar case than in the midlatitude case, in the 200\_2 run overcomes lower LWC in  
 732 the 200\_2 run than that in the 200\_0 run, which leads to the greater total cloud mass in the  
 733 200\_2 run than in the 200\_0 run (Figure 4 and Table 2). However, IWC whose magnitude  
 734 is similar to the magnitude of LWC, which results in a much lower IWC/LWC in the  
 735 midlatitude case than in the polar case, in the midlatitude case is not able to overcome  
 736 lower LWC in the midlatitude case than that in the midlatitude warm clouds, which leads  
 737 to the greater total cloud mass in the midlatitude warm clouds than in the midlatitude case;  
 738 here, the midlatitude warm clouds are generated by removing ice processes in the  
 739 midlatitude case. This means that associated with higher ICNC/CDNC and IWC/LWC, ice  
 740 processes enhance the total cloud mass for the polar case as compared to that for the polar

Formatted: Font: Not Italic

Formatted: Font: Not Italic

Deleted: This is

Deleted: 200\_2\_noise

Deleted: 200\_2\_noise

744 warm-cloud counterpart. However, in the midlatitude case, associated with lower  
 745 ICNC/CDNC and IWC/LWC, ice processes reduce the total cloud mass as compared to  
 746 that for the midlatitude warm-cloud counterpart.

747

### 748 **3.1.4, Role of ICNC/CDNC**

749

750 To test the hypothesis above about the role of ICNC/CDNC in above-described differences  
 751 between the polar and midlatitude cases, the 200\_2 run is repeated by reducing  
 752 ICNCavg/CDNCavg by a factor of 10. This is done by reducing the concentration of  
 753 aerosols acting as INP but not CCN in a way that ICNCavg/CDNCavg is lower by a factor  
 754 of 10 in the repeated run than in the 200\_2 run. In this way, this repeated run has  
 755 ICNCavg/CDNCavg at the same order of magnitude as that in the control-midlatitude run.

756 This repeated run is referred to as the 200\_0.07 run. As shown in Figure 8 and Table 2, the  
 757 200\_0.07 run shows much lower deposition rate and IWC than the 200\_2 run does.

758 However, as we move from the 200\_2 run to the 200\_0.07 run, the time- and domain-  
 759 averaged condensation rate and LWC increases (Figure 8 and Table 2). This is because

760 reduction in deposition increases the amount of water vapor, which is not consumed by  
 761 deposition but available for condensation. Associated with this, in the 200\_0.07 run, the

762 time- and domain-averaged deposition rate and IWC become similar to the average  
 763 condensation rate and LWC, respectively (Figure 8 and Table 2). Hence, IWC/LWC

764 reduces from 26.28 in the 200\_2 run to 1.05 in the 200\_0.07 run as ICNCavg/CDNCavg  
 765 reduces from the 200\_2 run to the 200\_0.07 run. Here, IWC/LWC in the 200\_0.07 run is

766 similar to that in the midlatitude-control run, which demonstrate that the difference in  
 767 ICNC/CDNC is able to explain the difference in IWC/LWC between the polar and

768 midlatitude cases. It is notable that the reduction in deposition is dominant over the increase  
 769 in condensation with the decrease in ICNCavg/CDNCavg. Hence, the sum of condensation

770 and deposition rates and WC reduce from the 200\_2 run to the 200\_0.07 run. That the sum  
 771 of condensation and deposition rates and WC reduce in a way that the sum and WC in the

772 mixed-phase clouds in the 200\_0.07 run are lower than condensation rate and LWC,  
 773 respectively, in the warm clouds in the 200\_0 run is also notable (Figure 8 and Table 2).

774 This is similar to the situation in the midlatitude case and thus demonstrates that the

Deleted: 2

Deleted: 200\_2\_fac10

Deleted: 6

Deleted: 200\_2\_fac10

Deleted: 200\_2\_fac10

Deleted: 6

Deleted: 200\_2\_fac10

Deleted: 6

Deleted: 200\_2\_fac10

Deleted: 200\_2\_fac10

Deleted: 200\_2\_fac10

Deleted: 200\_2\_fac10

Deleted: 2\_fac10

Deleted: 200\_2\_noise

Deleted: 6

790 different relation between the mixed-phase and warm clouds can be associated with the  
791 difference in ICNC/CDNC between the polar and midlatitude cases.

792 The rate of the sedimentation of ice crystals at the cloud base reduces as  
793 ICNCavg/CDNCavg reduces between the 200\_2 and 200\_0.07 runs, mainly due to  
794 reduction in the ice-crystal mass (Table 2). The rate of droplet sedimentation at the cloud  
795 base increases as ICNCavg/CDNCavg reduces mainly due to increases in droplet mass and  
796 size in association with the increases in LWC (Table 2). The entrainment rate at the cloud  
797 top reduces as ICNCavg/CDNCavg reduces (Table 2). It is found that those changes in the  
798 average rates of the droplet and ice-crystal sedimentation over the cloud base and  
799 simulation period are ~four to five orders of magnitude smaller than those in the average  
800 integrated condensation and deposition rates between the 200\_2 and 200\_0.07 runs (Table  
801 2). The entrainment tends to reduce the total cloud mass or WC less with the reducing  
802 ICNCavg/CDNCavg. Hence, changes in the entrainment counters the decrease in WC with  
803 the reducing ICNCavg/CDNCavg between the 200\_2 and 200\_0.07 runs. Here, we see that  
804 changes in the entrainment are not factors that lead to the increase in LWC, and the  
805 decrease in IWC, and eventually the decrease in WC with the reducing  
806 ICNCavg/CDNCavg. The analysis of the sedimentation and entrainment exclude them  
807 from factors inducing above-described differences between the 200\_2 and 200\_0.07 runs.  
808 Instead, this analysis grants confidence in the fact that deposition and condensation, which  
809 are strongly dependent on ICNC/CDNC, are main factors inducing those differences.

810

### 811 3.2 Aerosol-cloud interactions

812

813 Comparisons between the 200\_2 and 2000\_20 runs show that with the increasing  
814 concentration of both of aerosols acting as CCN and those as INP, IWC increases but LWC  
815 decreases in the polar case (Figures 9 and Table 2). These decreases in LWC are negligible  
816 as compared to these increases in IWC. Hence, the increases in IWC outweigh the  
817 decreases in LWC, leading to aerosol-induced increases in WC (Figures 9 and Table 2).  
818 To identify roles of specific types of aerosols in these aerosol-induced changes,  
819 comparisons not only between the 200\_2 and 200\_20 runs but also between the 200\_2 and  
820 2000\_2 runs are performed. Comparisons between the 200\_2 and 200\_20 runs show that

Deleted: 200\_2\_fac10

Deleted: Hence, the changing sedimentation tends to reduce LWC and increase IWC, while

Deleted: t

Deleted: changing

Deleted: increase

Deleted: changes in the sedimentation counter the increase in LWC, and the decrease in IWC with the reducing ICNCavg/CDNCavg. ...C

Deleted: C

Deleted: 200\_2\_fac10

Deleted: sedimentation and

Deleted: 200\_2\_fac10

Deleted: more

Deleted: 7

Deleted: 7

838 the increasing concentration of aerosols acting as INP induces increases in IWC but  
 839 decreases in LWC (Figure 9 and Table 2). The magnitudes of these increases and decreases  
 840 are similar to those between the 200\_2 and 2000\_20 runs (Figure 9 and Table 2). However,  
 841 comparisons between the 200\_2 and 2000\_2 runs show that the increasing concentration  
 842 of aerosols acting as CCN induces negligible changes in either IWC or LWC. Thus, CCN-  
 843 induced changes in the total cloud mass are negligible, although the increasing  
 844 concentration of aerosols acting as CCN induces a slight decrease in IWC, and a slight  
 845 increase in LWC (Figure 9 and Table 2). This demonstrates that INP plays a much more  
 846 important role than CCN when it comes to the response of the total cloud mass to increasing  
 847 aerosol concentrations. However, in the midlatitude case, the increasing concentration of  
 848 aerosols acting as CCN generates changes in the mass as significantly as the increasing  
 849 concentration of aerosols acting as INP does.

850 To identify roles played by ice processes in aerosol-cloud interactions, a pair of the  
 851 200\_0 and 2000\_0 runs are analyzed and compared to the previous four standard  
 852 simulations (i.e., the 200\_2, 200\_20, 2000\_2 and 2000\_20 runs). The CCN-induced  
 853 increases in LWC in those noise runs are much greater than the CCN-induced changes in  
 854 WC in the 200\_2 and 2000\_2 runs (Figure 9 and Table 2). However, these CCN-induced  
 855 increases in LWC in the noise runs are smaller than the INP-induced increases in WC in  
 856 the 200\_2 and 200\_20 runs (Figure 9 and Table 2). This is different from the midlatitude  
 857 case where changes in the total cloud mass, whether they are induced by the increasing  
 858 concentration of aerosols acting as CCN or INP, in the mixed-phase clouds are much lower  
 859 than those CCN-induced changes in the warm clouds.

860

### 861 3.2.1 Deposition, condensation, sedimentation and entrainment

862

863 The CCN-induced increases and decreases in condensation and deposition rates are  
 864 negligible, respectively. This leads to the CCN-induced negligible increases and decreases  
 865 in LWC and IWC, respectively, between the 200\_2 and 2000\_2 runs (Figure 9 and Table  
 866 2). However, between the 200\_2 and 200\_20 runs, rather the significant INP-induced  
 867 increases are in deposition rate, leading to the significant INP-induced increases in IWC  
 868 (Figure 9 and Table 2). Between the 200\_2 and 200\_20 runs, INP-induced decreases in

Deleted: 7

Deleted: 7

Deleted: 7

Deleted: 200\_2\_noise

Deleted: 2000\_2\_noise

Deleted: 7

Deleted: 7

Deleted: (

Deleted: )

Deleted: (

Deleted: )

Deleted: leading to

Deleted: (

Deleted: )

Deleted: (

Deleted: )

Deleted: 7

Deleted: 7

887 condensation rate are negligible, leading to the negligible INP-induced decreases in LWC,  
 888 as compared to the INP-induced increases in deposition rate and IWC (Figure 9 and Table  
 889 2). With the increasing concentration of aerosols acting as INP from the 200\_2 run to the  
 890 200\_20 run, the sedimentation of ice crystals at the cloud base decreases (Table 2). This is  
 891 mainly due to decreases in the size of ice crystals in association with increases INP and  
 892 resultant increases in ICNC. In Figure 10a, we see that the number concentration of ice  
 893 crystals with diameters smaller and larger than ~40 micron increases and decreases,  
 894 respectively, as we move from the 200\_2 run to the 200\_20 run, which indicate a shift of  
 895 the sizes of ice crystals to smaller ones. From the 200\_2 run to the 200\_20 run, the  
 896 sedimentation of droplets at the cloud base decreases as shown in Table 2, mainly due to  
 897 decreases in LWC. Figure 10b shows that the number concentration of drops decreases  
 898 throughout almost all parts of the size range from the 200\_2 run to the 200\_20 run, which  
 899 indicates a negligible shift in the drop size but a reduction in LWC. It is found that changes  
 900 in the average rates of the droplet and ice-crystal sedimentation over the cloud base and  
 901 simulation period are ~three to four orders of magnitude smaller than those in the average  
 902 integrated condensation and deposition rates between the 200\_2 and 200\_20 runs (Table  
 903 2). From the 200\_2 run to the 200\_20 run, the entrainment at the cloud top increases (Table  
 904 2). Hence, the entrainment reduces WC less in the 200\_2 run than in the 200\_20 run. Here,  
 905 we see that changes in entrainment and the sedimentation are not factors that we have to  
 906 focus on to explain the changes in LWC, IWC and WC between the 200\_2 and 200\_20  
 907 runs.

908 In the warm clouds in the 200\_0 and 2000\_0 runs, the CCN-induced increases in  
 909 condensation rate occur, leading to those in LWC (Figure 9 and Table 2). However, the  
 910 CCN-induced increases in condensation rate in the warm clouds associated with the polar  
 911 case are lower than the INP-induced increases in deposition rate in the polar case (Table  
 912 2). This contributes to aerosol-induced smaller changes in the total cloud mass in the polar  
 913 warm clouds than in the polar mixed-phase clouds. The sedimentation of droplets at the  
 914 cloud base reduces and the entrainment at the cloud top increases from the 200\_0 run to  
 915 2000\_0 run (Table 2). The increasing concentration of aerosols acting as CCN induces  
 916 increases in CDNC and decreases in the droplet size, leading to the reduction in the droplet  
 917 sedimentation from the 200\_0 run to 2000\_0 run. The entrainment counters the CCN-

Deleted: 7

Deleted:

Deleted: the INP-induced changes in the sedimentation contribute to the INP-induced increases in IWC but counter the INP-induced reduction in LWC. The entrainment counters the INP-induced increases in WC.

Deleted: nce

Deleted: droplet

Deleted: lead to the INP-induced increases in WC and decreases in LWC, respectively. The INP-induced increases in deposition and decreases in the sedimentation of ice crystals both contribute to the INP-induced increases in IWC. However, the INP-induced changes in the average integrated deposition rate over cloudy columns and the simulation period is ~ four orders of magnitude greater than those in the average rate of ice-crystal sedimentation over the cloud base and simulation period (Table 2). Hence, the role of the ice-crystal sedimentation in the INP-induced changes in IWC is negligible as compared to that of deposition.

Deleted: 200\_2\_noise

Deleted: 2000\_2\_noise

Deleted: 7

Deleted: 200\_2\_noise

Deleted: 2000\_2\_noise

Deleted: 200\_2\_noise

Deleted: 2000\_2\_noise

Deleted: The CCN-induced changes in the sedimentation contribute to the CCN-induced increases in LWC.

945 induced increases in LWC from the 200\_0 run to 2000\_0 run. Hence, the entrainment is  
 946 not a factor which induces the CCN-induced increases in LWC between the 200\_0 and  
 947 2000\_0 runs. As seen in Table 2, the changes in the sedimentation rate is ~three orders of  
 948 magnitude smaller than those in the integrated condensation rate between the 200\_0 and  
 949 2000\_0 runs. Hence, it is not the sedimentation but condensation that we have to look at to  
 950 explain changes in LWC or WC between the 200\_0 and 2000\_0 runs.

951

### 952 3.2.2 Understanding differences between the polar and midlatitude cases

953

954 Roughly speaking, the CCN-induced changes in LWC via CCN-induced changes in  
 955 autoconversion of droplets are proportional to LWC that changing CCN affect, and INP-  
 956 induced changes in IWC via INP-induced changes in autoconversion of ice crystals are  
 957 proportional to IWC that changing INPs affect (e.g., Dudhia, 1989; Murakami, 1990; Liu  
 958 and Daum, 2004; Morrison et al., 2005, 2009 and 2012; Lim and Hong, 2010; Mansell et  
 959 al. 2010; Kogan, 2013; Lee and Baik, 2017). This is for given environmental conditions  
 960 (e.g., temperature and humidity) and given CCN- or INP-induced changes in microphysical  
 961 factors such as sizes and number concentrations of droplets or ice crystals. Hence, in the  
 962 polar case, with a given much lower LWC than IWC, the changing concentration of  
 963 aerosols acting as CCN is likely to induce smaller changes in the given LWC via CCN  
 964 impacts on the droplet autoconversion. This is as compared to changes in the given IWC  
 965 which are induced by the changing concentration of aerosols acting as INP and thus  
 966 changing ice-crystal autoconversion.

967 The smaller changes in the given LWC are related to changes in CDNC. These changes  
 968 in CDNC are initiated by those in droplet autoconversion. The larger changes in the given  
 969 IWC are related to changes in ICNC. These changes in ICNC are initiated by those in ice-  
 970 crystal autoconversion. Changes in integrated droplet surface area, which are induced by  
 971 those in CDNC, initiate those in the given LWC. Changes in integrated ice-crystal surface  
 972 area, which are induced by those in ICNC, initiate those in the given IWC. Remember that  
 973 condensation occurs on droplet surface and thus droplets act as a source of condensation,  
 974 and deposition occurs on ice-crystal surface and thus ice crystals act as a source of  
 975 deposition. Hence, those changes in CDNC and associated integrated droplet surface area

Deleted: 200\_2\_noise

Deleted: 2000\_2\_noise

Deleted: the CCN-induced changes in

Deleted: are

Deleted: three

Deleted: .

Deleted: the role of

Deleted: in

Deleted: 200\_2\_noise

Deleted: 2000\_2\_noise

Deleted: is negligible as compared to that of condensation.

Formatted: Indent: Left: 1", No bullets or numbering

Formatted: Font: 12 pt, Not Bold, Font color: Text 1

Formatted: Line spacing: 1.5 lines

Formatted: Font: 12 pt, Not Bold, Font color: Text 1

Formatted: Font: 12 pt, Not Bold, Font color: Text 1



987 can lead to changes in condensation and thus feedbacks between condensation and updrafts,  
 988 while those changes in ICNC and associated integrated ice-crystal surface area can lead to  
 989 changes in deposition and thus feedbacks between deposition and updrafts. The smaller  
 990 CCN-induced changes in LWC involve changes in CDNC and associated smaller changes  
 991 in condensation and feedbacks between condensation and updrafts in the polar case. This  
 992 is as compared to changes in deposition and feedbacks between deposition and updrafts  
 993 which are associated with the INP-induced changes in ICNC and the related larger INP-  
 994 induced changes in IWC in the polar case. The smaller CCN-induced changes in LWC  
 995 involve smaller changes in water vapor that is consumed by droplets in the polar case. The  
 996 larger INP-induced changes in IWC involve larger changes in water vapor that is consumed  
 997 by ice crystals in the polar case. This leaves the CCN-induced smaller changes in the  
 998 amount of water vapor available for deposition, which induce the smaller CCN-induced  
 999 changes in IWC in the polar case. This is as compared to the INP-induced changes in the  
 1000 amount of water vapor which is available for condensation and associated changes in LWC  
 1001 in the polar case.

1002 ▼ The lower LWC in the polar warm clouds than IWC in the polar case contributes to the  
 1003 INP-induced greater changes in IWC than the CCN-induced changes in LWC in the polar  
 1004 warm clouds. The lower LWC in the polar case than that in the polar warm clouds  
 1005 contributes to the CCN-induced greater changes in LWC in the polar warm clouds than  
 1006 those in LWC and subsequent changes in IWC in the polar case.

1007 In contrast to the situation in the polar case, in the midlatitude case, remember that a  
 1008 given LWC is at the same order of magnitude of IWC. Hence, the CCN- induced changes  
 1009 in LWC and subsequent changes in IWC are similar to the INP-induced changes in IWC  
 1010 and subsequent changes in LWC. The greater LWC in the midlatitude warm cloud than  
 1011 both of LWC and IWC in the midlatitude case contributes to the greater CCN-induced  
 1012 changes in LWC in the midlatitude warm cloud. This is as compared to either the CCN-  
 1013 induced changes in LWC and subsequent changes in IWC or the INP-induced changes in  
 1014 IWC and subsequent changes in LWC in the midlatitude case.

1015 To confirm above-described mechanisms in this section, which explain different  
 1016 aerosol-cloud interactions between the polar and midlatitude cases, the 200\_0.07 run is  
 1017 repeated by increasing INP by a factor of 10 in the PBL at the first time step. This repeated

**Deleted:** Roughly speaking, the CCN-(INP-)induced changes in LWC (IWC) via CCN-(INP-)induced changes in autoconversion of droplets (ice crystals) are proportional to LWC (IWC) that changing CCN (INPs) affect (e.g., Liu and Daum, 2004; Kogan, 2013; Lee and Baik, 2017; Dudhia, 1989; Lim and Hong, 2010; Mansell et al. 2010). This is for given environmental conditions (e.g., temperature and humidity) and given CCN-(INP-)induced changes in microphysical factors such as sizes and number concentrations of droplets (ice crystals). Hence, in the polar case, with a given much lower LWC than IWC, the changing concentration of aerosols acting as CCN is likely to induce smaller changes in the given LWC via CCN impacts on the droplet autoconversion. This is as compared to changes in the given IWC which are induced by the changing concentration of aerosols acting as INP and thus changing ice-crystal autoconversion. ¶

The smaller (larger) changes in the given LWC (IWC) are related to changes in CDNC (ICNC). These changes in CDNC (ICNC) are initiated by those in droplet (ice crystal) autoconversion. Changes in integrated droplet (ice-crystal) surface area, which are induced by those in CDNC (ICNC), initiate those in the given LWC (IWC). Remember that condensation (deposition) occurs on droplet (ice-crystal) surface and thus droplets (ice crystals) act as a source of condensation (deposition). Hence, those changes in CDNC (ICNC) and associated integrated droplet (ice-crystal) surface area can lead to changes in condensation (deposition) and thus feedbacks between condensation (deposition) and updrafts. The smaller CCN-induced changes in LWC involve changes in CDNC and associated smaller changes in condensation and feedbacks between condensation and updrafts in the polar case. This is as compared to changes in deposition and feedbacks between deposition and updrafts which are associated with the INP-induced changes in ICNC and the related larger INP-induced changes in IWC in the polar case. The smaller CCN-induced changes in LWC involve smaller changes in water vapor that is consumed by droplets in the polar case. The larger INP-induced changes in IWC involve larger changes in water vapor that is consumed by ice crystals in the polar case. This leaves the CCN-induced smaller changes in the amount of water vapor available for deposition, which induce the smaller CCN-induced changes in IWC in the polar case. This is as compared to the INP-induced changes in the amount of water vapor which is available for condensation and associated changes in LWC in the polar case. ¶

**Deleted:** 200\_2\_fac10



run is referred to as “the 200 0.7 run. Then, the 200 0.07 run is repeated again by increasing CCN by a factor of 10 in the PBL at the first time step. This repeated run is referred to as the 2000 0.07 run. These repeated runs are to see the response of IWC and LWC to the increasing concentration of aerosols acting as INP and CCN. This is when IWC and LWC are at the same order of magnitude and lower in mixed-phase clouds than LWC in the warm-cloud counterpart as in the 200 0.07 run and midlatitude case. Comparisons between the 200 0.07, 200 0.7 and 2000 0.07 runs show that the INP-induced changes in IWC and LWC are similar to the CCN-induced changes in IWC and LWC, respectively, as in the midlatitude case (Figure 9 and Table 2). These comparisons also show that the CCN-induced changes in LWC in the polar warm cloud are greater (Figure 9 and Table 2). This is as compared to either the CCN-induced changes in LWC and subsequent changes in IWC between the 200 0.07 and 2000 0.07 runs or the INP-induced changes in IWC and subsequent changes in LWC between the 200 0.07 and 200 0.7 runs (Figure 9 and Table 2). These comparisons demonstrate that differences in ICNC/CDNC play a critical role in differences in aerosol-cloud interactions between the polar and midlatitude cases, considering that differences in ICNC/CDNC between the 200\_2 and 200 0.07 runs are at the same order of magnitude of those between the cases.

### 3.3 Radiation

Studies (e.g., Ovchinnikov et al., 2011; Possner et al., 2017; Solomon et al., 2018) have focused on radiative cooling and subsequent changes in stability and dynamics as a primary driver for the development of mixed-phase stratocumulus clouds and aerosol-induced changes in LWC and IWC in those clouds. Motivated by these studies, to isolate the role of radiative processes in cloud development and aerosol impacts on LWC and IWC, all of the simulations above are repeated by turning off radiative processes. In these repeated runs, radiative fluxes over the whole domain and simulation period are zero. The basic summary of results from these repeated runs is given in Table 3. As seen in comparisons between Tables 2 and 3, the qualitative nature of results, which are mainly about differences in IWC/LWC, the relative importance of the impacts of INP on IWC and LWC as compared to those impacts of CCN, and how warm and mixed-phase clouds are related

Deleted: 200\_2\_fac10\_INP10

Deleted: 200\_2\_fac10

Deleted: 200\_2\_fac10\_CCN10

Deleted: 200\_2\_fac10

Deleted: 200\_2\_fac10

Deleted: 200\_2\_fac10\_INP10

Deleted: 200\_2\_fac10\_CCN10

Deleted: .

Deleted: 200\_2\_fac10

Deleted: 200\_2\_fac10\_CCN10

Deleted: 200\_2\_fac10

Deleted: 200\_2\_fac10\_INP10

Deleted: 200\_2\_fac10

1104 between the polar and midlatitude cases, in this study does not vary with whether radiative  
1105 processes exist or not. This demonstrates that ICNC, CDNC, deposition and condensation  
1106 but not radiative processes drive results in this study.

1107

#### 1108 4. Discussion

1109

##### 1110 4.1 Examination of the role of ICNC/CDNC in IWC/LWC in 200\_2, 1111 2000\_20, 2000\_2, 200\_20, 200 0.07, 2000 0.07 and 200 0.7 runs

1112

1113 So far, comparisons between the set of the 200\_2, 2000\_20, 2000\_2 and 200\_20 runs for  
1114 the polar case and the other set of the 200 0.07, 2000 0.07 and 200 0.7 runs, which  
1115 represents the midlatitude case, have been mainly utilized to understand the role of  
1116 ICNC/CDNC. However, even when it comes to all the runs in both the sets, differences in  
1117 ICNCavg/CDNCavg and IWC/LWC are shown among them (Tables 1 and 2). For more  
1118 robust examination of particularly the role of ICNC/CDNC in IWC/LWC, which is  
1119 basically about the increase and decrease in ICNC/CDNC inducing the increase and  
1120 decrease in IWC/LWC, respectively, as identified from the comparison between the 200\_2  
1121 and 200 0.07 runs in Section 3.1.4, all the runs in the sets are utilized by ordering them as  
1122 shown in Table 4. This ordering is done in a way that as we move from the first run in the  
1123 first row to the last run in the last row of Table 4, ICNCavg/CDNCavg increases. Overall,  
1124 with increasing ICNCavg/CDNCavg, IWC/LWC increases, although the increase in  
1125 IWC/LWC is highly non-linear in terms of the increase in ICNCavg/CDNCavg as seen in  
1126 the percentage increases, and a decrease in IWC/LWC is seen with an increase in  
1127 ICNCavg/CDNCavg from the 2000\_20 run to the 200\_2 run (Table 4); this high-degree  
1128 non-linearity in the increase in IWC/LWC is associated with the fact that interactions  
1129 between cloud microphysical, thermodynamic and dynamic processes are well known to  
1130 be highly non-linear. Hence, overall, findings regarding the role of ICNC/CDNC in  
1131 IWC/LWC from the comparison between the 200\_2 and 200 0.07 runs are applicable to  
1132 all the runs in the sets except for the role between the 2000\_20 and 200\_2 runs. Here, it is  
1133 notable that the percentage difference in ICNCavg/CDNCavg is ~9% between the 2000\_20  
1134 and 200\_2 runs and the smallest among those differences in Table 4. The other differences

Deleted: 200\_2\_fac10  
Deleted: 200\_2\_fac10\_CCN10  
Deleted: 200\_2\_fac10\_INP10

Deleted: 200\_2\_fac10  
Deleted: 200\_2\_fac10\_CCN10  
Deleted: 200\_2\_fac10\_INP10

Deleted: (  
Deleted: )  
Deleted: (  
Deleted: )  
Deleted: 200\_2\_fac10  
Deleted: 2

Deleted:

Deleted: Hence,  
Deleted: o  
Deleted: 200\_2\_fac10

1151 are larger than 80%. Hence, the percentage difference in ICNCavg/CDNCavg for a pair of  
 1152 the 2000\_20 and 200\_2 runs is at least ~one order of magnitude smaller than that for the  
 1153 other pairs of the runs in Table 4. This means that findings from the comparison between  
 1154 the 200\_2 and 200\_0.07 runs are not suitable to explain the variation of IWC/LWC among  
 1155 clouds when the variation of ICNC/CDNC is relatively insignificant. According to Table  
 1156 4, it seems that the variation of ICNC/CDNC should be greater than a critical value above  
 1157 which those findings are useful to account for the IWC/LWC variation among clouds.

1158 ~~The high-degree non-linearity in the variation of IWC/LWC is epitomized by the 1706~~  
 1159 ~~percent increase in IWC/LWC for the 163 percent increase in ICNCavg/CDNCavg from~~  
 1160 ~~the 200\_0.7 run to the 2000\_2 run. This 1706 percent increase in IWC/LWC is induced by~~  
 1161 ~~increases in both the initial number concentrations of CCN and INP between the runs~~  
 1162 ~~(Table 1). In other transition from a simulation in a row to that in the next row in Table 4,~~  
 1163 ~~there are decreases in both the initial number concentrations of CCN and INP, or there is~~  
 1164 ~~either a change in the initial number condensation of CCN or INP. When either the initial~~  
 1165 ~~concentration of CCN or INP changes in the transition, less than a 100% increase in~~  
 1166 ~~IWC/LWC is shown. The decreases in both the initial number concentrations of CCN and~~  
 1167 ~~INP, which are from the 2000\_20 run to the 200\_2 run, result in the decrease in IWC/LWC.~~  
 1168 ~~Hence, depending on how the initial number concentrations of CCN and INP change, the~~  
 1169 ~~magnitude and sign of the change in IWC/LWC can vary substantially.~~

1170

#### 1171 **4.2 Role of a given ICNC/CDNC in IWC/LWC for different concentrations of** 1172 **aerosols acting as INP and CCN**

1173

1174 Simulations which are compared in Section 4.1 and shown in Table 4 have not only  
 1175 different ICNCavg/CDNCavg but also the different number concentrations of aerosols  
 1176 acting as CCN and INP at the first time step (Table 1). To better isolate particularly the  
 1177 role of ICNC/CDNC in IWC/LWC, we need to show that results in Section 4.1 are valid  
 1178 regardless of the variation of the number concentration of aerosols. For this need, we focus  
 1179 on the 200\_2 and 200\_0.07 runs, since the primary understanding of the role of  
 1180 ICNC/CDNC in IWC/LWC comes from the comparison between these runs as described  
 1181 in Section 3.1.4. To fulfill the need, each of these runs are repeated by varying the number

Deleted: 200\_2\_fac10

Formatted: Font: Not Italic

Formatted: Font: Not Italic

Formatted: Font: Not Italic

Formatted: Font: Not Italic

Formatted: Font: Not Italic

Formatted: Font: Not Italic

Formatted: Font: Not Italic

Formatted: Font: Not Italic

Formatted: Font: Not Italic

Deleted: 200\_2\_fac10

Deleted: 2

1185 concentration of aerosols acting as CCN and INP in a way that ICNCavg/CDNCavg does  
 1186 not vary (Tables 1 and 5). The 4000\_45 and 13\_0.1 runs are the repeated 200\_2 run, and  
 1187 the ~~4000\_1.8~~ and ~~12\_0.0035~~ runs are the repeated ~~200\_0.07~~ run (Tables 1 and 5). The set  
 1188 of the 200\_2, 4000\_45 and 13\_0.1 runs is referred to as the polar set, and that of the  
 1189 ~~200\_0.07~~, ~~4000\_1.8~~ and ~~12\_0.0035~~ runs is referred to as the midlatitude set in this section.  
 1190 Among the three runs in each of the sets, less than 4% variation of IWC/LWC is shown  
 1191 (Table 5). This less-than-4% variation is so small that the stark contrast in IWC/LWC  
 1192 between the 200\_2 and ~~200\_0.07~~ runs as discussed in Section 3.1.4 is also shown between  
 1193 the polar and midlatitude sets (Table 5). Hence, the role of the difference in a given  
 1194 ICNC/CDNC in the difference in IWC/LWC between the 200\_2 and ~~200\_0.07~~ runs as  
 1195 described in Section 3.1.4 is considered robust to the varying concentration of aerosols.

## 1197 5. Summary and conclusions

1198  
 1199 In this study, a case of mixed-phase stratiform clouds in a polar area, which is referred to  
 1200 as “the polar case” is compared to that in a midlatitude area, which is referred to as “the  
 1201 midlatitude case”. This is to gain an understanding of how different ICNC/CDNC plays a  
 1202 role in making differences in cloud properties, aerosol-cloud interactions and impacts of  
 1203 ice processes on them between two representative areas (i.e., polar and midlatitude areas)  
 1204 where mixed-phase stratiform clouds form and develop. Among those cloud properties,  
 1205 this study focuses on IWC/LWC that plays an important role in cloud radiative properties.  
 1206 To gain the understanding efficiently, the polar case is chosen in a way to make stark  
 1207 contrast with the midlatitude case in terms of ICNC/CDNC and IWC/LWC. Although such  
 1208 polar cases may be uncommon, the stark contrast provides an opportunity to elucidate  
 1209 mechanisms that control the above-mentioned role of different ICNC/CDNC.

1210 Due to lower air temperature, more ice crystals are nucleated, leading to higher  
 1211 ICNC/CDNC in the polar case than in the midlatitude case. This higher ICNC/CDNC  
 1212 enables the more efficient deposition of water vapor onto ice crystals in the polar case. This  
 1213 leads to much higher IWC/LWC in the polar case. The more efficient deposition of water  
 1214 vapor onto ice crystals enables the polar mixed-phase clouds to have the greater total cloud  
 1215 mass than the polar warm clouds. However, the less efficient deposition of water vapor

Deleted: 4000\_1.8\_fac10

Deleted: 12\_0.0035\_fac10

Deleted: 200\_2\_fac10

Deleted: 200\_2\_fac10

Deleted: 4000\_1.8\_fac10

Deleted: 12\_0.0035\_fac10

Deleted: 200\_2\_fac10

Deleted: 2

Deleted: 200\_2\_fac10

Deleted: 2

Deleted:

1227 onto ice crystals causes the midlatitude mixed-phase clouds to have less total cloud mass  
 1228 than the midlatitude warm clouds. With the increasing ICNC/CDNC from the midlatitude  
 1229 case to the polar case, impacts of CCN and INP on the total cloud mass become less and  
 1230 more important, respectively.

1231 This study picks ICNC/CDNC, which is affected by air temperature and its impacts on  
 1232 ice-crystal nucleation, as an important factor which differentiates IWC/LWC and  
 1233 interactions among clouds, aerosols and ice processes in the polar case from those in the  
 1234 midlatitude case. The polar case is located in the Svalbard area, which is in the Arctic,  
 1235 hence, more specifically, the polar case can be referred to as the Arctic case. Differences

1236 in ICNC/CDNC initiate differences in the microphysical properties (e.g., the integrated  
 1237 surface area), and then, subsequently induce those in thermodynamic latent-heat processes  
 1238 (e.g., condensation and deposition), dynamics of clouds, IWC/LWC and interactions  
 1239 among clouds, aerosols and ice processes. However, this does not mean that no other  
 1240 potential factors, which can explain the variation of IWC/LWC and interactions among  
 1241 clouds, aerosols and ice processes between different clouds, exist. For example, differences  
 1242 in environmental factors (e.g., stability and wind shear) between those different clouds can  
 1243 have an impact on the variation. Particularly, differences in stability and wind shear can  
 1244 initiate those in the dynamic development of turbulence. Then, this subsequently induces  
 1245 differences in the microphysical and thermodynamic development of clouds, IWC/LWC  
 1246 and interactions among clouds, aerosols and ice processes. Hence, factors such as stability  
 1247 and wind shear can have different orders of procedures, which involve dynamics,  
 1248 thermodynamics and microphysics, than ICNC/CDNC in terms of differentiation between  
 1249 different clouds. Thus, different mechanisms controlling the differentiation can be  
 1250 expected regarding factors such as stability and wind shear as compared to ICNC/CDNC.

1251 The examination of these different mechanisms among stability, wind shear and  
 1252 ICNC/CDNC deserves future study for more comprehensive understanding of the  
 1253 differentiation or for an above-mentioned more fully established general principle  
 1254 explaining the differentiation. Another point to make is that the cases in this study have  
 1255 weak precipitation and the associated weak sedimentation of ice crystals and droplets. In  
 1256 mixed-phase clouds with strong precipitation and the sedimentation, they can play roles as  
 1257 important as in-cloud latent-heat processes in IWC/LWC and interactions among clouds,

Deleted: (

Deleted: F

Deleted: )

Deleted: (

Deleted: )

Deleted: .

Deleted: ed

Deleted: area

Deleted: area

Deleted:

Deleted: those

Deleted: areas

Deleted: he areas

Deleted: the polar and midlatitude mixed-phase

Deleted: ¶

1274 aerosols and ice processes. In those clouds with strong precipitation, the sedimentation can  
1275 take part in the interplay between ICNC/CDNC and latent-heat processes by affecting  
1276 cloud mass and associated ICNC and CDNC significantly, and play a role in the  
1277 differentiation of IWC/LWC and interactions among clouds, aerosols and ice processes  
1278 when it comes to different cases of mixed-phase clouds. For more generalization of results  
1279 here as a way to the more fully established general principle, this potential role of  
1280 sedimentation needs to be investigated by performing more case studies involving cases  
1281 with strong precipitation in the future.

1282 It should be emphasized that although this study mentions air temperature as a factor  
1283 that affects ICNC/CDNC, ICNC/CDNC can be affected by other factors such as sources of  
1284 aerosols acting as INP and those acting as CCN, and/or the advection of those aerosols.  
1285 Hence, even for cloud systems that develop with a similar air-temperature condition, for  
1286 example, when those systems are affected by different sources of aerosols and/or their  
1287 different advection, they are likely to have different ICNC/CDNC, IWC/LWC, relative  
1288 importance of impacts of INP on IWC and LWC as compared to those impacts of CCN,  
1289 and relation between warm and mixed-phase clouds. Regarding factors, which affect  
1290 ICNC/CDNC, such as sources and advection of aerosols together with temperature , it  
1291 should be noted that while this study utilizes differences in temperature among those  
1292 factors to identify cases exhibiting significant disparities in ICNC/CDNC, its primary  
1293 objective does not lie in the role of temperature differences in disparities in ICNC/CDNC,  
1294 but in comprehending the inherent role of ICNC/CDNC variations themselves in the  
1295 discrepancies observed, for example, in IWC/LWC, across diverse cloud systems.

1296 Previous studies on mixed-phase stratocumulus clouds (e.g., Ovchinnikov et al., 2011;  
1297 Possner et al., 2017; Solomon et al., 2018) have primarily focused on investigating the  
1298 impacts of cloud-top radiative cooling, entrainment, and sedimentation of ice particles on  
1299 these clouds, as well as their interactions with aerosols. However, there are a scarcity of  
1300 studies that specifically examine the role of microphysical interactions, involving  
1301 processes such as condensation and deposition, as well as factors like cloud-particle  
1302 concentrations, between ice and liquid particles in mixed-phase stratocumulus clouds, and  
1303 their interactions with aerosols as performed in this study. Therefore, our study contributes

Deleted:

1305 to a more comprehensive understanding of mixed-phase clouds and their intricate interplay  
1306 with aerosols.

1307 This study suggests that a microphysical factor, which is ICNC/CDNC, can be a  
1308 simplified and useful tool to understand differences among different systems of  
1309 stratocumulus clouds in various regions in terms of IWC/LWC and the relative importance  
1310 of INP and CCN in aerosol-cloud interactions, and thus to contribute to the development  
1311 of general parameterizations of those clouds in various regions for climate models. This  
1312 factor can also be a useful tool for a simplified understanding of different roles of ice  
1313 processes when mixed-phase clouds are compared to their warm-cloud counterparts in  
1314 terms of the cloud development and its interactions with aerosols among those different  
1315 systems. It should be noted that warm clouds have been studied much more than mixed-  
1316 phase clouds, although mixed-phase clouds play as important roles as warm clouds in the  
1317 evolution of climate and its change. This study provides preliminary mechanisms which  
1318 differentiate mixed-phase clouds and their interactions with aerosols from their warm-  
1319 cloud counterparts, and control the variation of the differentiation in different regions as a  
1320 way of improving our understanding of mixed-phase clouds. It should be mentioned that  
1321 the efficient way of developing general parameterizations, which are for climate models  
1322 and consider all of warm, mixed-phase clouds in various regions and their interactions with  
1323 aerosols, can be achieved by just adding those mechanisms to pre-existing  
1324 parameterizations of much-studied warm clouds instead of developing brand new  
1325 parameterizations from the scratch.

1326 This study finds that the relation between ICNC/CDNC and IWC/LWC is highly non-  
1327 linear. This high non-linearity is closely linked to how the number concentrations of CCN  
1328 and INP, and associated ICNC/CDNC change. For a specific situation where the  
1329 ICNC/CDNC variation is relatively small and both the number concentrations of CCN and  
1330 INP reduce, the increase in ICNC/CDNC can reduce IWC/LWC, although it is found that  
1331 as a whole, the increase in ICNC/CDNC enhances IWC/LWC. Hence, mechanisms  
1332 identified in this study, especially regarding the use of ICNC/CDNC as a simplified and  
1333 useful tool to explain differences in IWC/LWC among different cloud systems, are not  
1334 complete and entirely general. In addition, results in this study are from only two cases in  
1335 two specific locations in the midlatitude and Arctic regions and the more generalization of

Deleted: ,

Deleted:

Deleted:

Deleted: although those

Deleted:

Deleted: may not be

Deleted: , they can act as a valuable building block that can streamline the development of those general parameterizations.

Deleted:

1345 these results in this study merits more case studies over more locations in those regions,  
1346 for example, in terms of above-mentioned sedimentation intensity, different factors (e.g.,  
1347 environmental factors) other than ICNC/CDNC, different sources and advection of  
1348 aerosols, the magnitude of the variation of ICNC/CDNC and the way number  
1349 concentrations of CCN and INP vary. Hence, findings particularly about relations between  
1350 ICNC/CDNC and IWC/LWC in this study should be considered preliminary ones that  
1351 initiate future work to streamline the development of the general parameterizations.

1352

1353

1354

1355

1356

1357

1358

1359

1360

1361

1362

1363

1364

1365

1366

1367

1368

1369

1370

1371

1372

1373

1374

1375



1376 **Code/Data source and availability**

1377

1378 Our private computer system stores the code/data which are private and used in this study.

1379 Upon approval from funding sources, the data will be opened to the public. Projects related

1380 to this paper have not been finished, thus, the sources prevent the data from being open to

1381 the public currently. However, if information on the data is needed, contact the

1382 corresponding author Seoung Soo Lee (slee1247@umd.edu).

1383

1384 **Author contributions**

1385 Essential initiative ideas are provided by SSL, CHJ and YJY to start this work. Simulation

1386 and observation data are analyzed by SSL, CHJ and JU. YZ, JP, MGM and SKS review

1387 the results and contribute to their improvement. JC provides supports to set up and run

1388 additional simulations during the review.

1389

1390 **Competing interests**

1391 The authors declare that they have no conflict of interest.

1392

1393 **Acknowledgements**

1394 This study is supported by the National Research Foundation of Korea (NRF) grant funded

1395 by the Korea government (MSIT) (Nos. NRF2020R1A2C1003215,

1396 NRF2020R1A2C2011081, NRF2023R1A2C1002367,

1397 NRF2021M1A5A1065672/KOPRI-PN23011 and 2020R1A2C1013278), and Basic

1398 Science Research Program through the NRF funded by the Ministry of Education (No.

1399 2020R1A6A1A03044834).

1400

1401

1402

1403

1404

1405

1406

1407

1408

1409 **References**

- 1410  
1411 Ackerman, A., Kirkpatrick, M., Stevens, D., et al.: The impact of humidity above  
1412 stratiform clouds on indirect aerosol climate forcing, *Science*, 432, 1014–1017,  
1413 <https://doi.org/10.1038/nature03174>, 2004.
- 1414 Albrecht, B. A.: Aerosols, cloud microphysics, and fractional cloudiness, *Science*, 245,  
1415 1227–1230, 1989.
- 1416 Bartosiewicz, Y., and Duponcheel, M.: Large eddy simulation: Application to liquid metal  
1417 fluid flow and heat transfer . In: Roelofs, Ferry, *Thermal Hydraulics Aspects of Liquid*  
1418 *Metal Cooled Nuclear Reactors*, Woodhead Publishing, 2018.
- 1419 Brown, A., Milton, S., Cullen, M., Golding, B., Mitchell, J., and Shelly, A.: Unified  
1420 modeling and prediction of weather and climate: A 25-year journey, *B. Am. Meteorol.*  
1421 *Soc.*, 93, 1865–1877, 2012.
- 1422 Chen, F., and Dudhia, J.: Coupling an advanced land-surface hydrology model with the  
1423 Penn State-NCAR MM5 modeling system. Part I: Model description and  
1424 implementation, *Mon. Wea. Rev.*, 129, 569–585, 2001.
- 1425 Choi, Y.-S., Ho, C.-H., Park, C.-E., Storelvmo, T., and Tan, I.: Influence of cloud phase  
1426 composition on climate feedbacks, *J. Geophys. Res.*, 119, 3687–3700,  
1427 doi:10.1002/2013JD020582, 2014.
- 1428 Choi, Y.-S., Lindzen, R. S., Ho, C.-H., and Kim, J.: Space observations of cold-cloud phase  
1429 change, *Proc. Natl. Acad. Sci. U.S.A.*, 107, 11211–11216, 2010
- 1430 Chua, X. R., and Ming, Y.: Convective invigoration traced to warm-rain microphysics,  
1431 *Geophys. Res. Lett.*, 47, <https://doi.org/10.1029/2020GL089134>, 2020.
- 1432 Dione, C., Lohou, F., Lothon, M., Adler, B., Babić, K., Kalthoff, N., Pedruzo-Bagazgoitia,  
1433 X., Bezombes, Y., and Gabella, O.: Low-level stratiform clouds and dynamical  
1434 features observed within the southern West African monsoon, *Atmos. Chem. Phys.*,  
1435 19, 8979–8997, <https://doi.org/10.5194/acp-19-8979-2019>, 2019.
- 1436 Donovan, D. P.: Ice-cloud effective particle size parameterization based on combined lidar,  
1437 radar reflectivity, and mean Doppler velocity measurements, *J. Geophys. Res.*, 108,  
1438 4573, doi:10.1029/2003JD003469, 2003.
- 1439 [Donovan, D. P., and van Lammeren, A. C. A. P.: Cloud effective particle size and water](#)

Deleted: ,

- 1441 [content profile retrievals using combined lidar and radar observations: 1. Theory and](#)  
 1442 [examples, J. Geophys. Res., 106, 27,425–27,448, 2001.](#)
- 1443 Donovan, D. P., van Lammeren, A.C.A.P., Hogan, R. J., Russchenberg, H. W. J., Apituley,  
 1444 A., Francis, P., Testud, J., Pelon, J., Quante, M., and Goddard, J. W. F.: Cloud effective  
 1445 particle size and water content profile retrievals using combined lidar and radar  
 1446 observations – 2. Comparison with IR radiometer and in situ measurements of ice  
 1447 clouds, J. Geophys. Res, 106, 27449-27464, 2001.
- 1448 Dudhia, J.: Nemerical study of convection observed during the winter monsoon  
 1449 Experiment using a mesoscale two-dimensional Model, J. Atmos. Sci., 46, 3077–3107,  
 1450 <https://doi.org/10.1175/1520-0469>, 1989.
- 1451 Fan, J., Rosenfeld, D., Zhang, Y., Giangrande, S. E., Li, Z., Machado, L. A. T., Martin, S.  
 1452 T., Yang, Y., Wang, J., and Artaxo, P.: Substantial convection and precipitation  
 1453 enhancements by ultrafine aerosol particles. Science, 359, 411–418, 2018
- 1454 Forster, P., et al., Changes in atmospheric constituents and in radiative forcing, in: Climate  
 1455 change 2007: the physical science basis, Contribution of working group I to the Fourth  
 1456 Assessment Report of the Intergovernmental Panel on Climate Change, edited by  
 1457 Solomon, S., et al., Cambridge Univ. Press, New York, 2007.
- 1458 [Gettelman, A., Liu, X., Barahona, D., et al.: Climate impacts of ice nucleation, J. Geophys.](#)  
 1459 [Res., 117, D20201, doi:10.1029/2012JD017950, 2012.](#)
- 1460 [Gras, J. L.: Southern hemisphere tropospheric aerosol microphysics, J. Geophys. Res., 96,](#)  
 1461 [5345-5356.](#)
- 1462 Hahn, C. J., and Warren, S. G.: A gridded climatology of clouds over land (1971–96) and  
 1463 ocean (1954–97) from surface observations worldwide, Numeric Data Package NDP-  
 1464 026EORNL/CDIAC-153, CDIAC, Department of Energy, Oak Ridge, TN, 2007.
- 1465 Hannak, L., Knippertz, P., Fink, A. H., Kniffka, A., and Pante, G.: Why do global climate  
 1466 models struggle to represent low-level clouds in the West African summer monsoon?,  
 1467 J. Climate, 30, 1665–1687, <https://doi.org/10.1175/JCLI-D-16-0451.1>, 2017
- 1468 Hartmann, D. L., Ockert-Bell, M. E., and Michelsen, M. L.: The effect of cloud type on  
 1469 earth's energy balance—Global analysis, J. Climate, 5, 1281–1304, 1992.
- 1470 Hartmann, M., Gong, X., Kecorius, S., van Pinxteren, M., Vogl, T., Welti, A., Wex, H.,  
 1471 Zeppenfeld, S., Herrmann, H., Wiedensohler, A., and Stratmann, F.: Terrestrial or

Deleted: ,

Formatted: Font: Not Italic

Formatted: Font: Not Bold

- 1473 marine – indications towards the origin of ice-nucleating particles during melt season  
1474 in the European Arctic up to 83.7° N, *Atmos. Chem. Phys.*, 21, 11613–11636,  
1475 <https://doi.org/10.5194/acp-21-11613-2021>, 2021.
- 1476 Hogan, R. J., Illingworth, A. J., O'Connor, E. J., et al.: Cloudnet: Evaluation of model  
1477 clouds using ground-based observations, ECMWF Workshop on parametrization of  
1478 clouds on large-scale models., 2006.
- 1479 IPCC: Climate Change: The Physical Science Basis. Contribution of Working Group I to  
1480 the Sixth Assessment Report of the Intergovernmental Panel on Climate Change  
1481 [Masson-Delmotte, V., Zhai, P., Pirani, A., Connors, S. L., Péan, C., Berger, S., Caud,  
1482 N., Chen, Y., Goldfarb, L., Gomis, M. I., Huang, M., Leitzell, K., Lonnoy, E.,  
1483 Matthews, J. B. R., Maycock, T. K., Waterfield, T., Yelekçi, O., Yu, R., and Zhou, B.  
1484 (eds.)]. Cambridge University Press, Cambridge, United Kingdom and New York, NY,  
1485 USA, In press, doi:10.1017/9781009157896, 2021.
- 1486 [Jaenicke, R.: Tropospheric aerosols in Aerosol-Cloud-Climate Interactions, Hobbs, P. V.,](#)  
1487 [ed., Academic Press, San Diego, CA, pp. 1-31.](#)
- 1488 [Jiang, H., Feingold, G. and Cotton, W. R.: Simulations of aerosol-cloud-dynamical](#)  
1489 [feedbacks resulting from entrainment of aerosol into the marine boundary layer during](#)  
1490 [the Atlantic Stratocumulus Transition Experiment, \*J. Geophys. Res.\*, 107\(D24\), 4813,](#)  
1491 [doi:10.1029/2001JD001502, 2002.](#)
- 1492 Jung, C. H., Yoon, Y. J., Kang, H. J., Gim, Y., Lee, B. Y., Ström, J., Krejci, R., and Tunved,  
1493 P.: The seasonal characteristics of cloud condensation nuclei (CCN) in the arctic lower  
1494 troposphere, *Tellus B: Chemical and Physical Meteorology*, 70:1, 1513291, [https://doi:](https://doi:10.1080/16000889.2018.1513291)  
1495 [10.1080/16000889.2018.1513291](https://doi:10.1080/16000889.2018.1513291), 2018.
- 1496 Khain, A. P., Ovchinnikov, M., Pinsky, M., Pokrovsky, A. and Krugliak, H.: Notes on the  
1497 state-of-the-art numerical modeling of cloud microphysics, *Atmos. Res.*, 55, 159–224,  
1498 2000.
- 1499 Khain, A., Pokrovsky, A., Rosenfeld, D., Blahak, U., and Ryzhkov, A.: The role of CCN in  
1500 precipitation and hail in a mid-latitude storm as seen in simulations using a spectral  
1501 (bin) microphysics model in a 2D dynamic frame, *Atmos. Res.*, 99, 129–146, 2011.
- 1502 Khain, A. P., Phillips, V., Benmoshe, N., Pokrovsky, A.: The role of small soluble aerosols  
1503 in the microphysics of deep maritime clouds, *J. Atmos. Sci.*, 69, 2787–2807, 2012.

- 1504 Knippertz, P., Fink, A. H., Schuster, R., Trentmann, J., Schrage, J. M., and Yorke, C.: Ultra-  
 1505 low clouds over the southern West African monsoon region, *Geophys. Res. Lett.*, 38,  
 1506 L21808, <https://doi.org/10.1029/2011GL049278>, 2011.
- 1507 Kogan, Y., 2013: A cumulus cloud microphysics parameterization for cloud-resolving  
 1508 models, *J. Atmos. Sci.*, 70, 1423–1436, <https://doi:10.1175/JAS-D-12-0183.1>, 2013.
- 1509 Koop, T., Luo, B. P., Tsias, A., and Peter, T.: Water activity as the determinant for  
 1510 homogeneous ice nucleation in aqueous solutions, *Nature*, 406, 611–614.
- 1511 Lee, H., and Baik, J.-J.: A physically based autoconversion parameterization, *J. Atmos. Sci.*,  
 1512 74, 1599–1616, <https://doi.org/10.1175/JAS-D-16-0207.1>, 2017.
- 1513 Lee S. S., Penner, J. E., and Saleeby, S. M.: Aerosol effects on liquid-water path of thin  
 1514 stratocumulus clouds, *J. Geophys. Res.*, 114, D07204, doi:10.1029/2008JD010513,  
 1515 2009.
- 1516 Lee, S. S., et al., Mid-latitude mixed-phase stratocumulus clouds and their interactions with  
 1517 aerosols: how ice processes affect microphysical, dynamic and thermodynamic  
 1518 development in those clouds and interactions?, *Atmos. Chem. Phys.*,  
 1519 <https://doi.org/10.5194/acp-21-16843-2021>, 2021.
- 1520 Li, J., Carlson, B. E., Yung, Y. L., Lv, D., Hansen, J., Penner, J. E., Liao, H., Ramaswamy,  
 1521 V., Kahn, R. A., Zhang, P., Dubovik, O., Ding, A., Lacis, A. A., Zhang, L., and Dong,  
 1522 Y.: Scattering and absorbing aerosols in the climate system, *Nature Reviews Earth and*  
 1523 *Environment*, 3, 363–379, <https://doi.org/10.1038/s43017-022-00296-7>, 2022.
- 1524 Lilly, D. K.: The representation of small scale turbulence in numerical simulation  
 1525 experiments, *Proc. Ibm Sci. Comput. Symp. Environ. Sci.*, 320–1951, 195–210, 1967.
- 1526 Lim, K.-S. S., and Hong, S.-Y.: Development of an effective double-moment cloud  
 1527 microphysics scheme with prognostic cloud condensation nuclei (CCN) for weather  
 1528 and climate models, *Mon. Wea. Rev.*, 138, 1587–1612,  
 1529 doi:10.1175/2009MWR2968.1., 2010.
- 1530 Liu, Y., and Daum, P. H.: Parameterization of the autoconversion. Part I: Analytical  
 1531 formulation of the Kessler-type parameterizations, *J. Atmos. Sci.*, 61, 1539–1548,  
 1532 doi:10.1175/1520-0469(2004)061,1539:POTAPI.2.0.CO;2, 2004.
- 1533 Lohmann, U., and Diehl, K.: Sensitivity studies of the importance of dust ice nuclei for  
 1534 the indirect aerosol effect on stratiform mixed-phase clouds, *J. Atmos. Sci.*, 63, 968–

Deleted: 2022

- 1536 982, 2006.
- 1537 Mansell, E. R., Ziegler, C. L., and Bruning, E. C., Simulated electrification of a small  
1538 thunderstorm with two-moment bulk microphysics, *J. Atmos. Sci.*, 67, 171–194,  
1539 doi:10.1175/2009JAS2965.1., 2010.
- 1540 Ming, Y., and Chua, X. R.: Convective invigoration traced to warm-rain microphysics,  
1541 *Geophys. Res. Lett.*, 47, doi.org/10.1029/2020GL089134, 2020.
- 1542 Mlawer, E. J., Taubman, S. J., Brown, P. D., Iacono, M. J., and Clough, S. A.: RRTM, a  
1543 validated correlated-k model for the longwave, *J. Geophys. Res.*, 102, 16663–1668,  
1544 1997.
- 1545 [Moeng, C.-H., Sullivan, P. P., and Stevens, B.: Including radiative effects in an entrainment  
1546 rate formula for buoyancy-driven PBLs, \*J. Atmos. Sci.\*, 56, 1031 – 1049,  
1547 doi:10.1175/1520-0469\(1999\)056<1031:IREIAE>2.0.CO;2, 1999.](#)
- 1548 Möhler, O., et al, Efficiency of the deposition mode ice nucleation on mineral dustparticles,  
1549 *Atmos. Chem. Phys.*, 6, 3007–3021, 2006.
- 1550 [Morrison, H., deBoer, G., Feingold, G., Harrington, J., Shupe, M., and Sulia, K., Resilience  
1551 of persistent Arctic mixed-phase clouds, \*Nat. Geosci.\*, 5, 11–17,  
1552 https://doi.org/10.1038/ngeo1332, 2012.](#)
- 1553 [Morrison, H., Curry, J. A., and Khvorostyanov, V. I., A new double-moment microphysics  
1554 parameterization for application in cloud and climate models. Part I: Description, \*J.\*  
1555 \*Atmos. Sci.\*, 62, 1665–1677, 2005.](#)
- 1556 [Morrison, H., hompson, G., and V. Tatarskii, Impact of cloud microphysics on the  
1557 development of trailing stratiform precipitation in a simulated squall line: Comparison  
1558 of one- and two-moment schemes. \*Mon. Wea. Rev.\*, 137, 991–1007,  
1559 https://doi.org/10.1175/2008MWR2556.1., 2009.](#)
- 1560 [Murakami, M., 1990, Numerical modeling of the dynamical and microphysical evolution  
1561 of an isolated convective cloud—The July 19 1981 CCOPE cloud, \*J. Meteor. Soc.\*  
1562 \*Japan\*, 68, 107–128.](#)
- 1563 Ovchinnikov, M., Korolev, A., and Fan, J.: Effects of ice number concentration on  
1564 dynamics of a shallow mixed-phase stratiform cloud, *J. Geophys. Res.*, 116, D00T06,  
1565 doi:10.1029/2011JD015888, 2011.
- 1566 Possner, A., Ekman, A. M. L., and Lohmann, U.: Cloud response and feedback processes

Deleted: ¶

- 1568 in stratiform mixed-phase clouds perturbed by ship exhaust, *Geophys. Res. Lett.*, 44,  
 1569 1964–1972, <https://doi.org/10.1002/2016GL071358>, 2017.
- 1570 Pruppacher, H. R. and Klett, J. D.: *Microphysics of clouds and precipitation*, 714pp, D.  
 1571 Reidel, 1978.
- 1572 Ramaswamy, V., et al.: Radiative forcing of climate change, in *Climate Change 2001: The*  
 1573 *Scientific Basis*, edited by J. T. Houghton et al., 349-416, Cambridge Univ. Press,  
 1574 New York, 2001.
- 1575 [Seinfeld, J. H., and Pandis, S. N.: \*Atmospheric chemistry and physics: From air pollution\*](#)  
 1576 [to climate change, John Wiley & Sons, 1326 pp, 1998.](#)
- 1577 Solomon, A., de Boer, G., Creamean, J. M., McComiskey, A., Shupe, M. D., Maahn, M.,  
 1578 and Cox, C.: The relative impact of cloud condensation nuclei and ice nucleating  
 1579 particle concentrations on phase partitioning in Arctic mixed-phase stratocumulus  
 1580 clouds, *Atmos. Chem. Phys.*, 18, 17047–17059, [https://doi.org/10.5194/acp-18-](https://doi.org/10.5194/acp-18-17047-2018)  
 1581 [17047-2018](https://doi.org/10.5194/acp-18-17047-2018), 2018.
- 1582 Smagorinsky, J.: General circulation experiments with the primitive equations, *Mon. Wea.*  
 1583 *Rev.*, 91, 99–164, 1963.
- 1584 [Stevens, B., et al.: On entrainment rates in nocturnal marine stratocumulus, \*Q. J. R. Meteorol. Soc.\*, 129, 3469 – 3492, doi:10.1256/qj.02.202, 2003a.](#)
- 1585 [Stevens, B., et al.: Dynamics and chemistry of marine stratocumulus-DYCOMS-II, \*Bull. Am. Meteorol. Soc.\*, 84, 579– 593, doi:10.1175/BAMS-84-5-579, 2003b.](#)
- 1586 [Stevens, B., and Feingold, G.: Untangling aerosol effects on clouds and precipitation in a](#)  
 1587 [buffered system, \*Nature\*, 461, 607–613, <https://doi.org/10.1038/nature08281>, 2009.](#)
- 1588 Stephens, G. L., and Greenwald, T. J.: Observations of the Earth's radiation budget in  
 1589 relation to atmospheric hydrology. Part II: Cloud effects and cloud feedback, *J.*  
 1590 *Geophys. Res.*, 96, 15 325–15 340, 1991.
- 1591 Tinel, C., Testud, J., Hogan, R. J., Protat, A., Delanoe, J. and Bouniol, D.: The retrieval of  
 1592 ice cloud properties from cloud radar and lidar synergy, *J. Appl. Meteorol.*, 44, 860-  
 1593 875, 2005.
- 1594 [Tsushima, Y., Webb, M. J., Williams, K. D., Soden, B. J., et al.: Importance of the mixed-](#)  
 1595 [phase cloud distribution in the control climate for assessing the response of clouds to](#)  
 1596 [carbon dioxide increase: A multi-model study, \*Clim. Dyn.\*, 27, 113–126, 2006.](#)

Deleted: ¶

1600 Tunved, P., Ström, J. and Krejci, R.: Arctic aerosol life cycle: linking aerosol size  
1601 distributions observed between 2000 and 2010 with air mass transport and  
1602 precipitation at Zeppelin station, Ny-Ålesund, Svalbard, *Atmos. Chem. Phys.*,  
1603 13, 3643–3660, <https://doi:10.5194/acp-13-3643-2013>, 2013

1604 Twomey, S.: Pollution and the Planetary Albedo, *Atmos. Env.*, 8,1251-1256, 1974.

1605 Warren, S. G., Hahn, C. J., London, J., Chervin, R. M., and Jenne, R. L.: Global distribution  
1606 of total cloud cover and cloud types over land, NCAR Tech. Note NCAR/TN-  
1607 273+STR, National Center for Atmospheric Research, Boulder, CO, 29 pp. + 200  
1608 maps, 1986.

1609 Wood, R.: Stratocumulus clouds, *Mon. Wea. Rev.*, 140, 2373-2423, 2012.

1610 [Xue, L., Teller, A., Rasmussen, R. M., Geresdi, I., and Pan, Z.: Effects of aerosol solubility  
1611 and regeneration on warm-phase orographic clouds and precipitation simulated by a  
1612 detailed bin microphysical scheme, \*J. Atmos. Sci.\*, 67, 3336–3354, 2010.](#)

1613 Zhang, D., Vogelmann, A., Kollias, P., Luke, E., Yang, F., Lubin, D., and Wang, Z.:  
1614 Comparison of Antarctic and Arctic single-layer stratiform mixed-phase cloud  
1615 properties using ground-based remote sensing measurements, *J. Geophys. Res.*, 124,  
1616 10186–10204, <https://doi.org/10.1029/2019JD030673>, 2019.

1617 Zheng, Y., Zhang, H., Rosenfeld, D., Lee, S. S., Su, T., and Li, Z.: Idealized Large-Eddy  
1618 Simulations of Stratocumulus Advecting over Cold Water. Part I: Boundary Layer  
1619 Decoupling, 78, 4089-4102, <https://doi.org/10.1175/JAS-D-21-0108.1>, 2021.

1620  
1621  
1622  
1623  
1624  
1625  
1626  
1627  
1628  
1629  
1630  
1631  
1632  
1633  
1634  
1635



1636 **FIGURE CAPTIONS**

1637

1638 Figure 1. A red rectangle marks the simulation domain in the Svalbard area, Norway. The  
1639 light blue represents the ocean and the green the land area.

1640

1641 Figure 2. (a) The vertical distributions of the domain-averaged potential temperature and  
1642 humidity at the first time step, (b) the time series of the domain-averaged large-scale  
1643 subsidence or downdraft at the model top and (c) the time series of the domain-averaged  
1644 surface temperature.

1645

1646 Figure 3. Aerosol size distribution at the surface. N represents aerosol number  
1647 concentration per unit volume of air and D represents aerosol diameter.

1648

1649 Figure 4. The vertical distributions of the time- and domain-averaged IWC and LWC in  
1650 the 200\_2 and 200\_0 runs.

1651

1652 Figure 5. The time series of (a) observed and simulated cloud-top and bottom heights, (b)  
1653 retrieved and simulated IWP, and observed and simulated LWP, and (c) the simulated  
1654 surface sensible and latent heat fluxes. For the time series, the simulated cloud-top height  
1655 is averaged over grid points with cloud tops and the simulated cloud-bottom height is  
1656 averaged over grid points with cloud bottoms, while the simulated IWP and LWP are  
1657 averaged over grid points with non-zero IWP and LWP, respectively, at each time step in  
1658 the 200\_2 run. The simulated surface sensible and latent heat fluxes are averaged over the  
1659 horizontal domain at the surface and each time step in the 200\_2 run.

1660

1661 Figure 6. The vertical distributions of the time- and domain-averaged deposition and  
1662 condensation rates in the 200\_2 and 200\_0 runs.

1663

1664 Figure 7. The time series of the average supersaturation with respect to ice and water over  
1665 grid points where deposition occurs in the presence of both droplets and ice crystals in the  
1666 200\_2 run.

Deleted: 1

Deleted: 200\_2\_noise

Deleted: 1

Deleted: 5

Deleted: 200\_2\_noise

1686  
1687  
1688  
1689  
1690  
1691  
1692  
1693  
1694  
1695  
1696  
1697  
1698  
1699  
1700  
1701  
1702  
1703  
1704  
1705  
1706  
1707  
1708  
1709  
1710  
1711  
1712  
1713  
1714  
1715  
1716

Figure 8. The vertical distributions of the time- and domain-averaged IWC and LWC in the 200\_2, 200\_0 and 200\_0.07 runs.

Figure 9. The vertical distributions of the time- and domain-averaged (a) IWC in the 200\_2, 2000\_20, 200\_0.07, 200\_20, 2000\_2, 2000\_0.07, and 200\_0.7 runs. (b) The vertical distributions of the time- and domain-averaged LWC in the 200\_0 and 2000\_0 runs as well as all the runs shown in panel (a).

Figure 10. The average size distributions of (a) ice crystals over grid points with non-zero IWC and the simulation period and (b) drops over grid points with non-zero LWC and the simulation period.

Deleted: 6

Deleted: 200\_2\_noise

Deleted: 200\_2\_fac10

Deleted: 7

Deleted: 200\_2\_fac10

Deleted: 200\_2\_fac10\_CCN10

Deleted: 200\_2\_fac10\_INP10

Deleted: 200\_2\_noise

Deleted: 2000\_2\_noise

Deleted: ,

Deleted:

Deleted: 1

Simulations	The number concentration of aerosols acting as CCN at the first time step in the PBL (cm <sup>-3</sup> )	The number concentration of aerosols acting as INP at the first time step in the PBL (cm <sup>-3</sup> )	ICNCavg/CDNCavg	Ice processes	Formatted Table
200 2	200	2	0.220	Present	Present
2000 20	2000	20	0.201	Present	Present
2000 2	2000	2	0.108	Present	Present
200 20	200	20	0.512	Present	Present
200 0	200	2	0.000	Absent	Deleted: 2_noice
2000 0	2000	2	0.000	Absent	Deleted: 2_noice
200 0.07	200	0.07	0.022	Present	Deleted: 2_fac10
2000 0.07	2000	0.07	0.012	Present	Deleted: 2_fac10_CCN10
200 0.7	200	0.7	0.041	Present	Deleted: 2_
4000 45	4000	45	0.220	Present	Deleted: fac10_INP10
13 0.1	13	0.1	0.220	Present	Deleted: 200_2_norad
4000 1.8	4000	1.8	0.022	Present	Deleted: fac10
12 0.0035	12	0.0035	0.022	Present	Deleted: 5_fac10

1729

1730 Table 1. Summary of simulations

1731

1732

1733

1734

1735

1736

1737

1738

1739

1740

1741

1742

1743

1744

1745

1746

Simulations	IWC (10 <sup>3</sup> g m <sup>-3</sup> )	LWC (10 <sup>3</sup> g m <sup>-3</sup> )	IWP (g m <sup>-2</sup> )	LWP (g m <sup>-2</sup> )	IWC/LWC	IWP/LWP	Condensation rate		Deposition rate		Cloud-base sedimentation (10 <sup>-3</sup> g m <sup>-2</sup> s <sup>-1</sup> )		Entrainment (cm s <sup>-1</sup> )
							Over grid points (10 <sup>-2</sup> g m <sup>-3</sup> s <sup>-1</sup> )	Over cloudy columns ( g m <sup>-2</sup> s <sup>-1</sup> )	Over grid points (10 <sup>-2</sup> g m <sup>-3</sup> s <sup>-1</sup> )	Over cloudy columns ( g m <sup>-2</sup> s <sup>-1</sup> )	Ice- crystal	Droplet	
200_2	6.57	0.25	31.94	1.23	26.28	25.96	0.11	1.98	1.30	23.40	1.17	0.17	0.25
2000_20	7.82	0.21	40.91	1.08	37.24	37.91	0.09	1.62	1.57	28.26	0.94	0.06	0.53
2000_2	6.55	0.29	31.85	1.46	22.58	21.81	0.12	2.16	1.28	23.04	1.11	0.08	0.28
200_20	7.80	0.20	40.82	1.01	39.00	40.42	0.09	1.62	1.56	28.08	0.97	0.11	0.51
<del>200_0</del>	0.00	2.06	0.00	10.35	0.00	0.00	0.72	12.48	0.00	0.00	0.00	0.36	
<del>2000_0</del>	0.00	2.25	0.00	11.29	0.00	0.00	0.76	12.80	0.00	0.00	0.00	0.14	
<del>200_0.07</del>	0.89	0.85	4.27	4.20	1.05	1.02	0.32	5.76	0.35	6.30	0.19	0.28	
<del>2000_0.07</del>	0.79	0.97	3.82	4.83	0.81	0.79	0.38	6.84	0.31	5.58	0.17	0.19	
<del>200_0.7</del>	0.98	0.78	4.73	3.88	1.25	1.22	0.31	5.58	0.39	7.02	0.14	0.22	

**Deleted: 200\_2\_noise**

**Deleted: 2000\_2\_noise**

**Deleted: 200\_2\_fac10**

**Deleted: 200\_2\_fac10\_CCN10**

**Deleted: 200\_2\_fac10\_INP10**

1756

1757

1758

1759

1760

1761

1762

1763

1764

1765

1766

1767

1768

1769

1770

1771

1772

1773

1774

1775

1776

1777

1778

Table 2. The averaged IWC, LWC, IWP, LWP, condensation and deposition rates over all of grid points and the simulation period in each of simulations. IWC/LWC (IWP/LWP) is the averaged IWC (IWP) over the averaged LWC (LWP). Also, as shown are the vertically integrated condensation and deposition rates over each cloudy column which are averaged over those columns and the simulation period. The average cloud-base sedimentation rate, which is for each of ice crystals and droplets, over the cloud base and simulation period, and the average cloud-top entrainment rate over the cloud top and simulation period are shown as well.

Simulations	IWC (10 <sup>3</sup> g m <sup>-3</sup> )	LWC (10 <sup>3</sup> g m <sup>-3</sup> )	IWP (g m <sup>-2</sup> )	LWP (g m <sup>-2</sup> )	IWC/LWC	IWP/LWP	Condensation rate		Deposition rate		Cloud-base sedimentation (10 <sup>-3</sup> g m <sup>-2</sup> s <sup>-1</sup> )		Entrainment (cm s <sup>-1</sup> )
							Over grid points (10 <sup>2</sup> g m <sup>-3</sup> s <sup>-1</sup> )	Over cloudy columns ( g m <sup>-2</sup> s <sup>-1</sup> )	Over grid points (10 <sup>2</sup> g m <sup>-3</sup> s <sup>-1</sup> )	Over cloudy columns ( g m <sup>-2</sup> s <sup>-1</sup> )	Ice- crystal	Droplet	
							200_2_norad	6.42	0.24	31.21	1.22	26.75	
2000_20_norad	7.63	0.21	40.05	1.07	36.33	37.42	0.09	1.59	1.55	29.91	0.92	0.06	0.51
2000_2_norad	6.40	0.29	31.11	1.45	22.06	21.45	0.11	2.12	1.26	22.69	1.07	0.08	0.27
200_20_norad	7.61	0.20	39.95	0.99	38.05	40.35	0.09	1.59	1.54	27.72	0.97	0.11	0.49
200_0_norad	0.00	2.03	0.00	10.20	0.00	0.00	0.72	12.31	0.00	0.00	0.00	0.34	
2000_0_norad	0.00	2.21	0.00	11.12	0.00	0.00	0.75	12.63	0.00	0.00	0.00	0.13	
200_0.07_norad	0.87	0.84	4.21	4.17	1.04	1.01	0.31	5.74	0.35	6.21	0.18	0.27	
2000_0.07_norad	0.78	0.96	3.78	4.80	0.81	0.79	0.36	6.81	0.30	5.50	0.16	0.18	
200_0.7_norad	0.97	0.76	4.70	3.85	1.25	1.22	0.30	5.55	0.38	6.91	0.13	0.21	

Deleted: 200\_2\_noise

Deleted: 2000\_2\_noise

Deleted: 200\_2\_fac10

Deleted: 200\_2\_fac10\_CCN10

Deleted: 200\_2\_fac10\_INP10

1784

1785 Table 3. Same as Table 2 but for the repeated simulations with radiative processes turned  
1786 off.

1787

1788

1789

1790

1791

1792

1793

1794

1795

1796

1797

1798

1799

1800

1801

1802

1803

1804

1805

1806

Simulations	ICNCavg/CDNCavg	Percentage increases (+) or decrease (-) in ICNCavg/CDNCavg	IWC/LWC	Percentage increases (+) or decrease (-) in IWC/LWC
<del>2000 0.07</del>	0.012		0.81	
<del>200 0.07</del>	0.022	+83.33%	1.05	+29.6%
<del>200 0.7</del>	0.041	+86.36%	1.25	+19.0%
2000 2	0.108	+163.4%	22.58	+1706.4%
2000 20	0.201	+86.1%	37.24	+64.9%
200 2	0.220	+9.4%	26.28	-29.4%
200 20	0.512	+132.7%	39.00	+48.4%

Deleted: 200\_2\_fac10\_CCN10

Deleted: 200\_2\_fac10

Deleted: 200\_2\_fac10\_INP10

1812

1813 Table 4. ICNCavg/CDNCavg and IWC/LWC in the simulations that are related to Section  
 1814 4.1. The Percentage increases or decreases in ICNCavg/CDNCavg and IWC/LWC as  
 1815 shown in the  $i^{\text{th}}$  row are  $\frac{(\text{ICNCavg/CDNCavg})_i - (\text{ICNCavg/CDNCavg})_{i-1}}{(\text{ICNCavg/CDNCavg})_{i-1}} \times 100$  (%) and  
 1816  $\frac{(\text{IWC/LWC})_i - (\text{IWC/LWC})_{i-1}}{(\text{IWC/LWC})_{i-1}} \times 100$  (%), respectively. Here,  $(\text{ICNCavg/CDNCavg})_i$  and  
 1817  $(\text{IWC/LWC})_i$  represent ICNCavg/CDNCavg and IWC/LWC in the  $i^{\text{th}}$  row, respectively.

1818

1819

1820

1821

1822

1823

1824

1825

1826

1827

1828

1829

1830

1831

1832

1833

Deleted: ¶

¶

Simulations	ICNCavg/CDNCavg	IWC/LWC	Percentage increases (+) or decrease (-) in IWC/LWC
Polar case			
200_2	0.220	26.28	
4000_45	0.220	27.25	+3.7%
13_0.1	0.220	25.62	-2.5%
Representing midlatitude case			
<del>200_0.07</del>	0.022	1.05	
<del>4000_1.8</del>	0.022	1.09	+3.8%
<del>12_0.0035</del>	0.022	1.02	-2.9%

Deleted: 200\_2\_fac10

Deleted: 4000\_1.8\_fac10

Deleted: 12\_0.0035\_fac10

1839

1840 Table 5. ICNCavg/CDNCavg and IWC/LWC in the simulations that are related to Section

1841 4.2. The percentage increases or decreases in IWC/LWC in the 4000\_45 run or in the

1842 13\_0.1 run are  $\frac{(IWC/LWC)_{4000\_45 \text{ or } 13\_0.1} - (IWC/LWC)_{200\_2}}{(IWC/LWC)_{200\_2}} \times 100 (\%)$ . Here,

1843  $(IWC/LWC)_{4000\_45 \text{ or } 13\_0.1}$  represents IWC/LWC in the 4000\_45 run or the 13\_01 run, while

1844  $(IWC/LWC)_{200\_2}$  represents IWC/LWC in the 200\_2 run. The percentage increases or

1845 decreases in IWC/LWC in the ~~4000\_1.8~~ run or the ~~12\_0.0035~~ run are

1846  $\frac{(IWC/LWC)_{4000\_1.8\_fac10 \text{ or } 12\_0.0035\_fac10} - (IWC/LWC)_{200\_2\_fac10}}{(IWC/LWC)_{200\_2\_fac10}} \times 100 (\%)$ . Here,

Deleted: 4000\_1.8\_fac10

Deleted: 12\_0.0035\_fac10

1847  $(IWC/LWC)_{4000\_1.8 \text{ or } 12\_0.0035}$  represents IWC/LWC in the ~~4000\_1.8~~ run or the ~~12\_0.0035~~

1848 run, while  $(IWC/LWC)_{200\_0.07}$  represents IWC/LWC in the ~~200\_0.07~~ run.

Deleted: 4000\_1.8\_fac10

Deleted: 12\_0.0035\_fac10

Deleted: 4000\_1.8\_fac10

Deleted: 12\_0.0035\_fac10

Deleted: 200\_2\_fac10

Deleted: 200\_2\_fac10

1849

1850

1851

1852

1853

1854

1855

1856

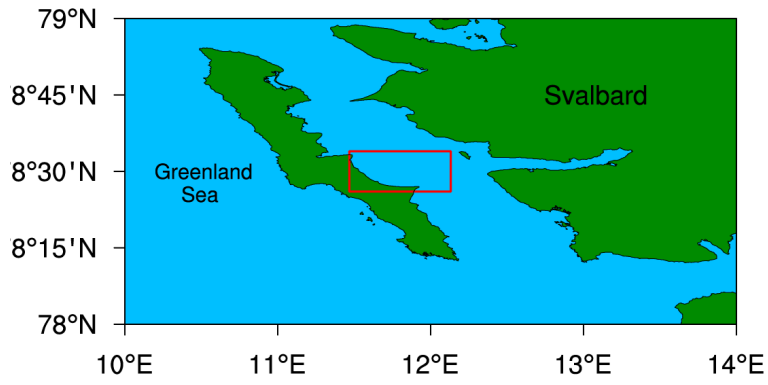
1857

1858

1859

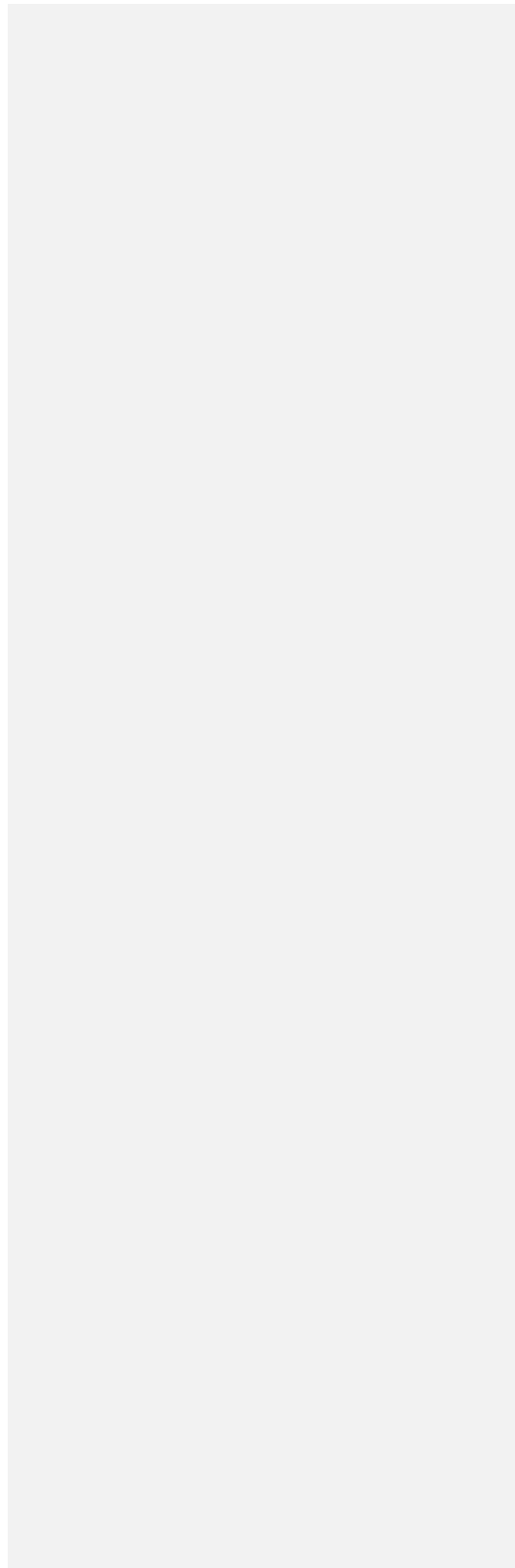
1860

1861

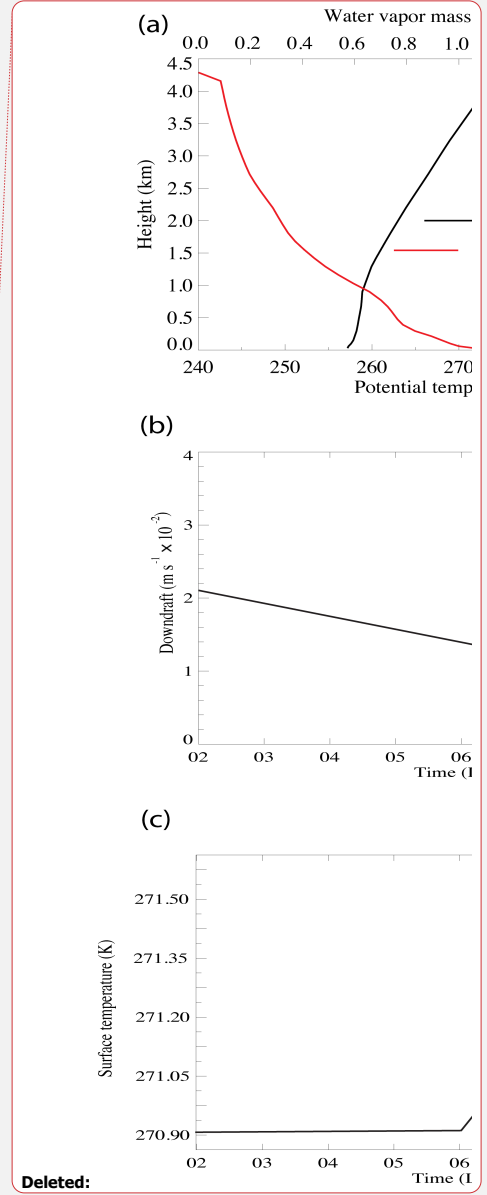
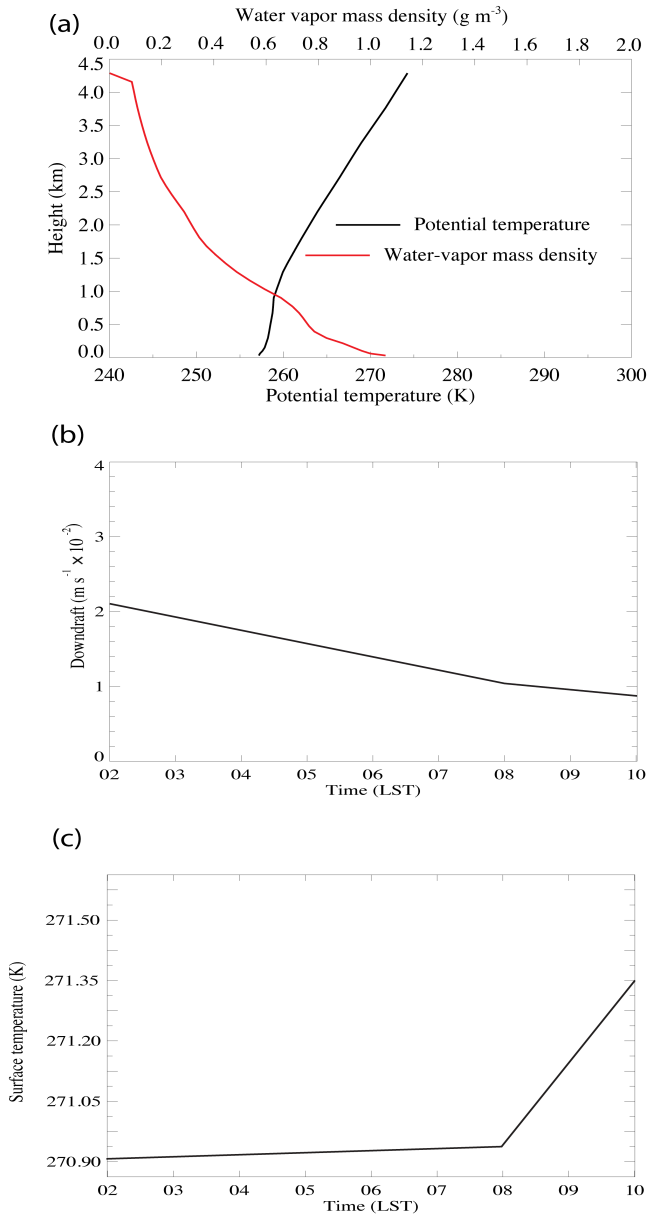


1873  
1874  
1875  
1876  
1877  
1878  
1879  
1880  
1881  
1882  
1883  
1884  
1885  
1886  
1887  
1888  
1889  
1890  
1891  
1892

**Figure 1**





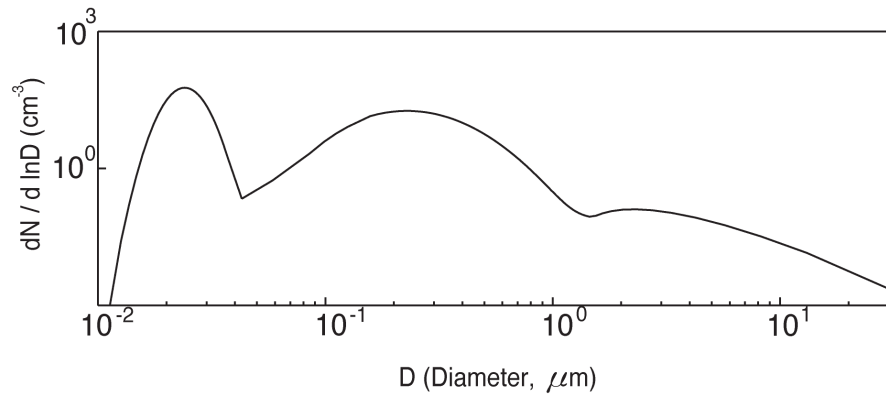


Deleted:

Figure 2

1893

1894

**Figure 3**

1896

1897

1898

1899

1900

1901

1902

1903

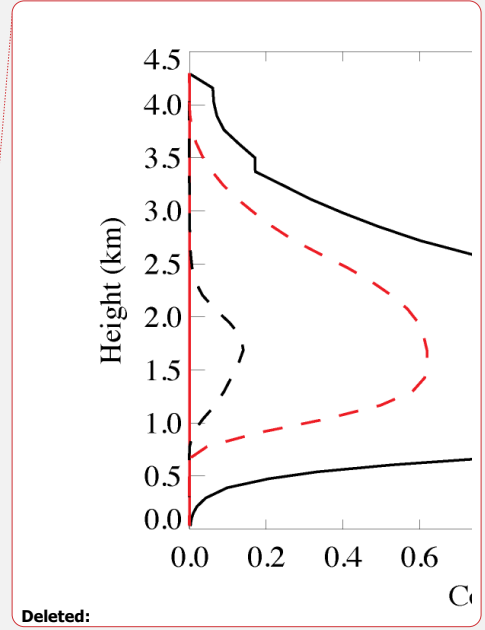
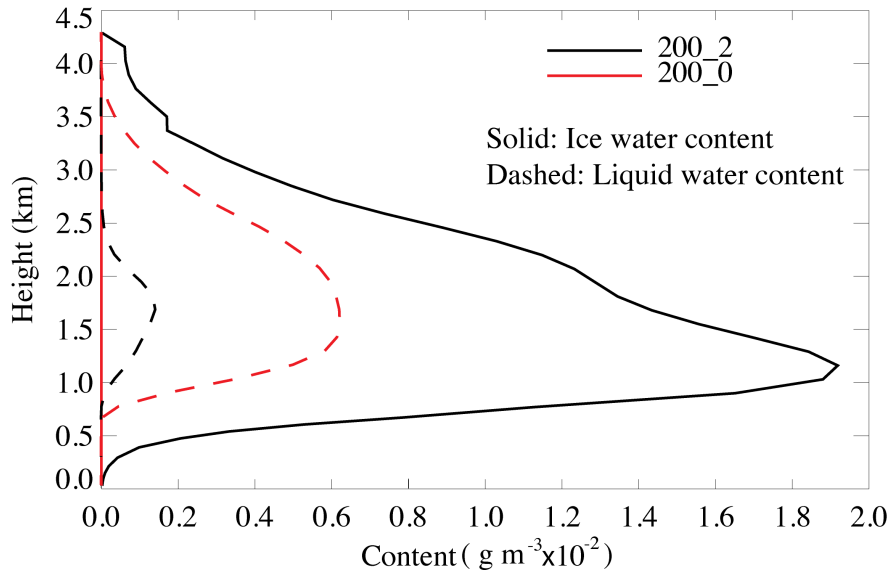
1904

1905

1906

1907

1908



Deleted:

1909

1910

1911

1912

1913

1914

1915

1916

1917

Figure 4

Deleted:

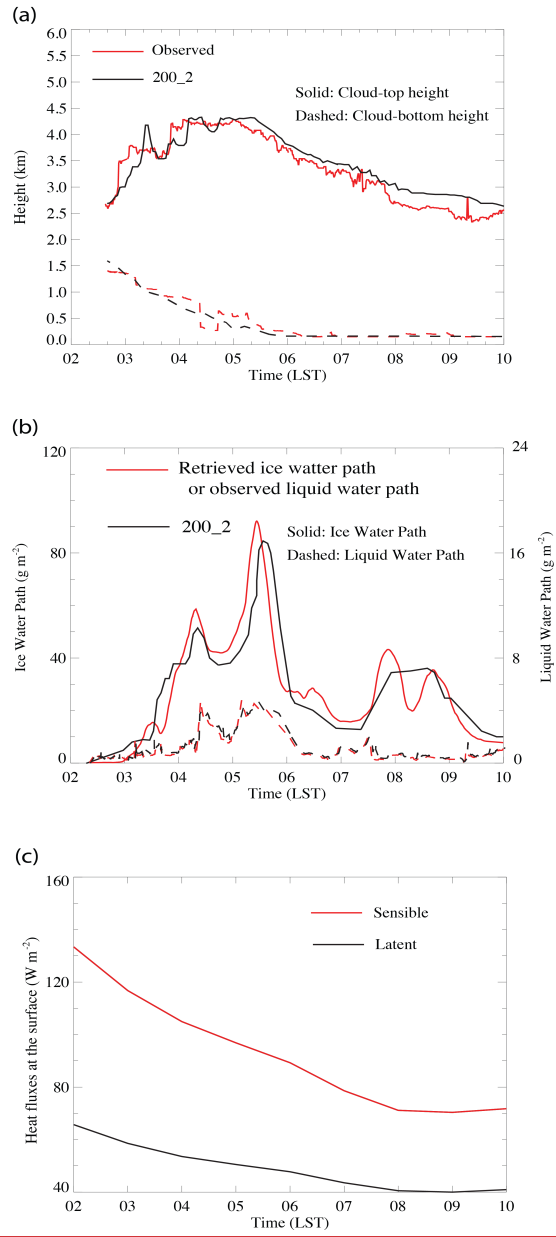
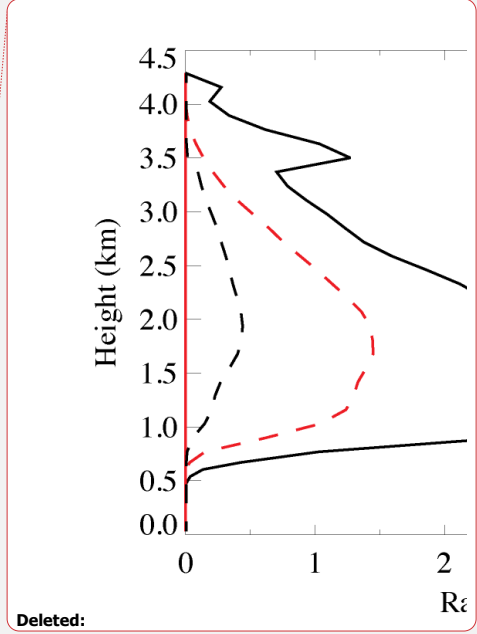
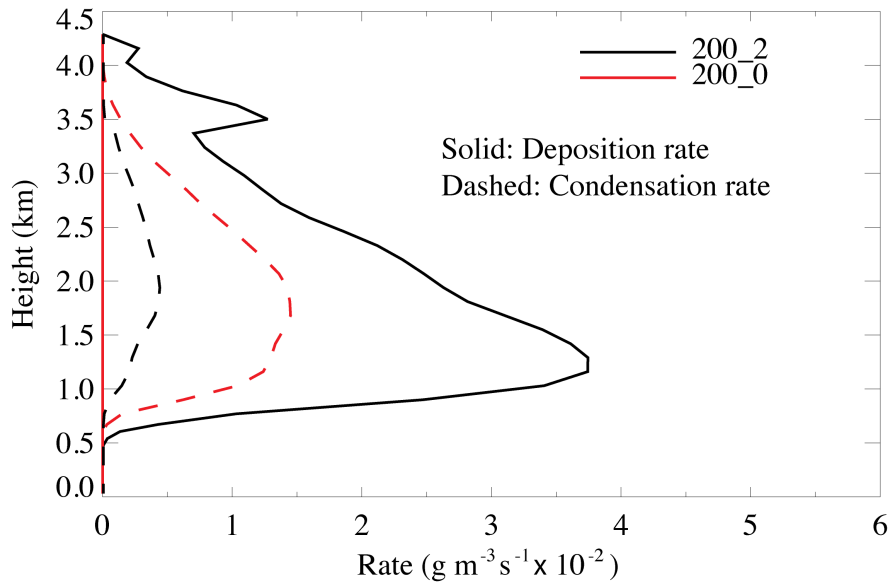


**Figure 5**

1920

1921



Deleted:

Deleted: 5

Figure 6

1922

1923

1924

1925

1926

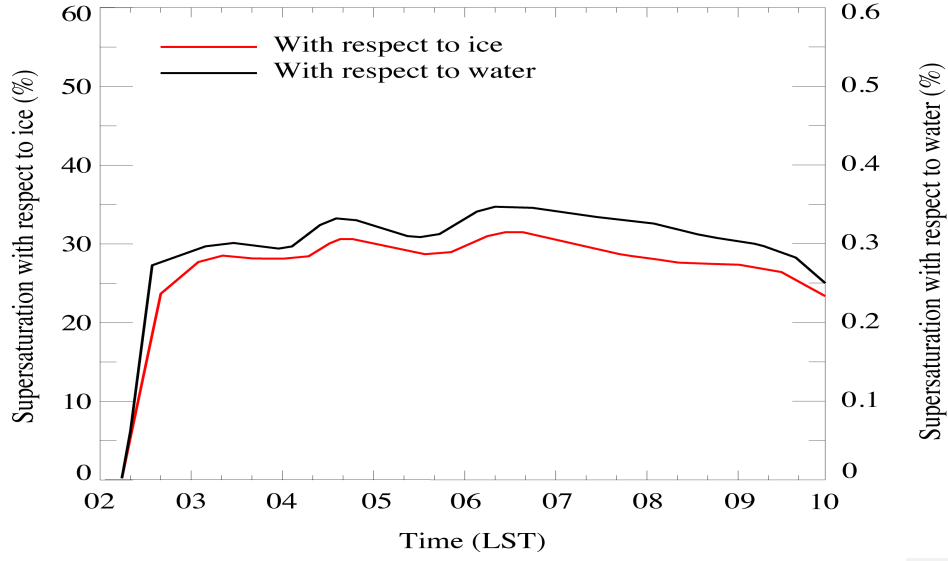
1927

1928

1929

1930

1931

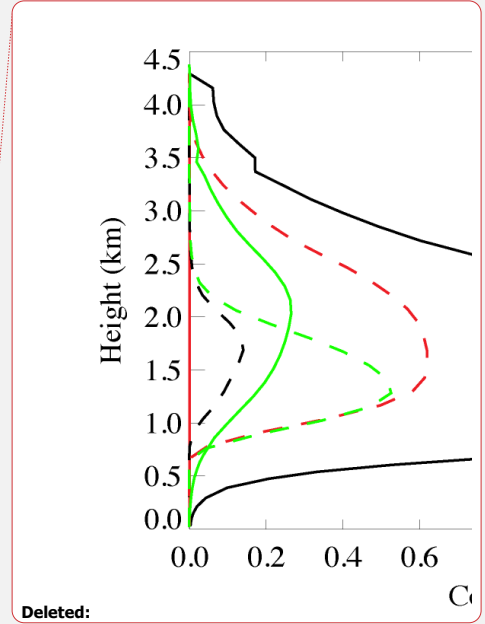
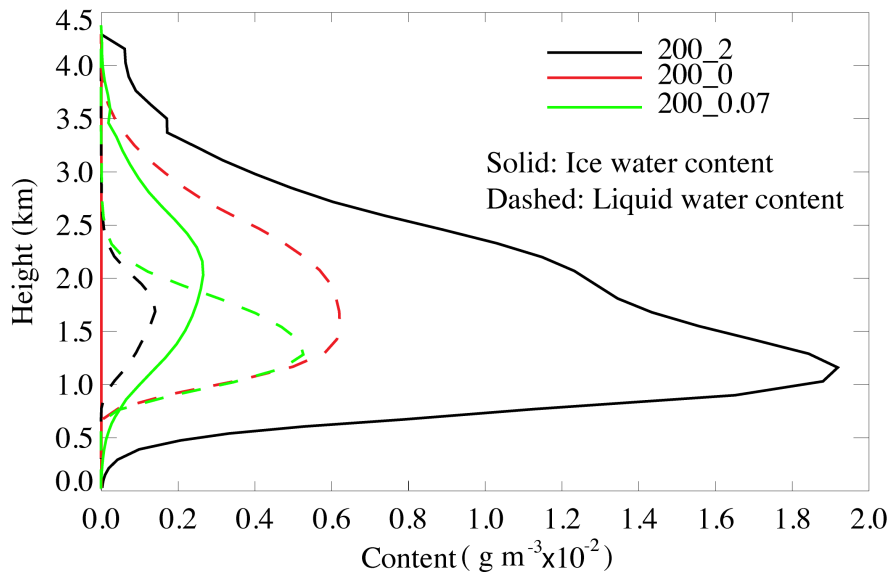


1934

1935

1936

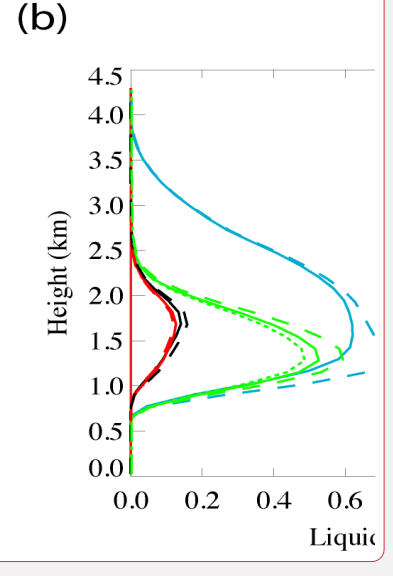
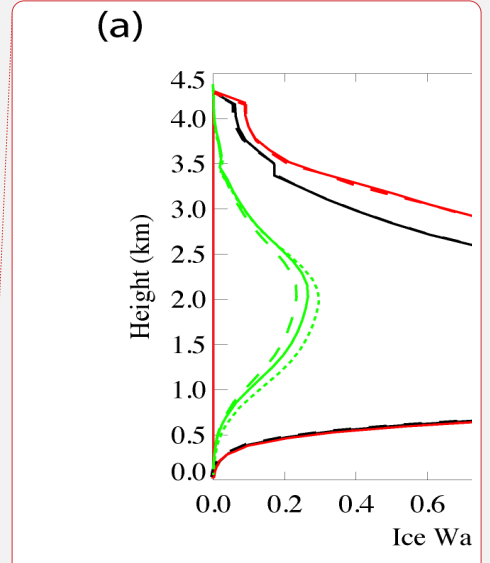
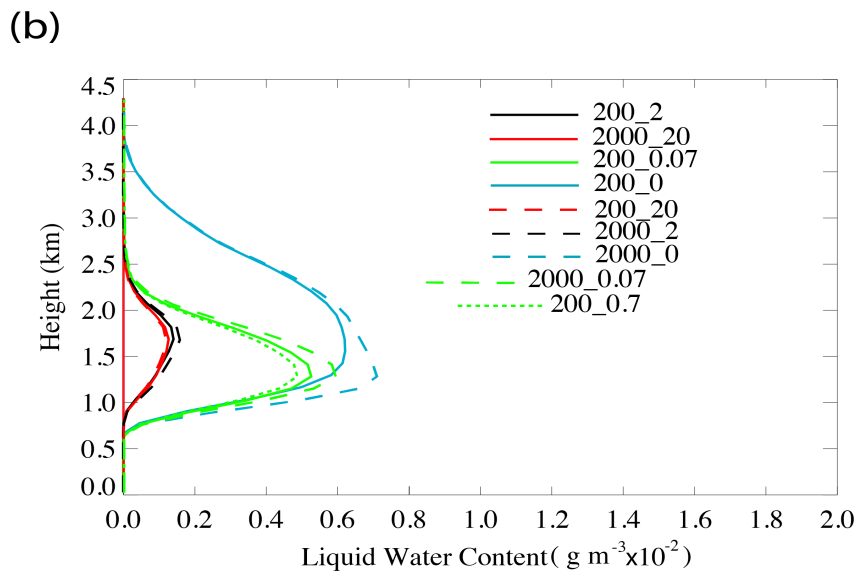
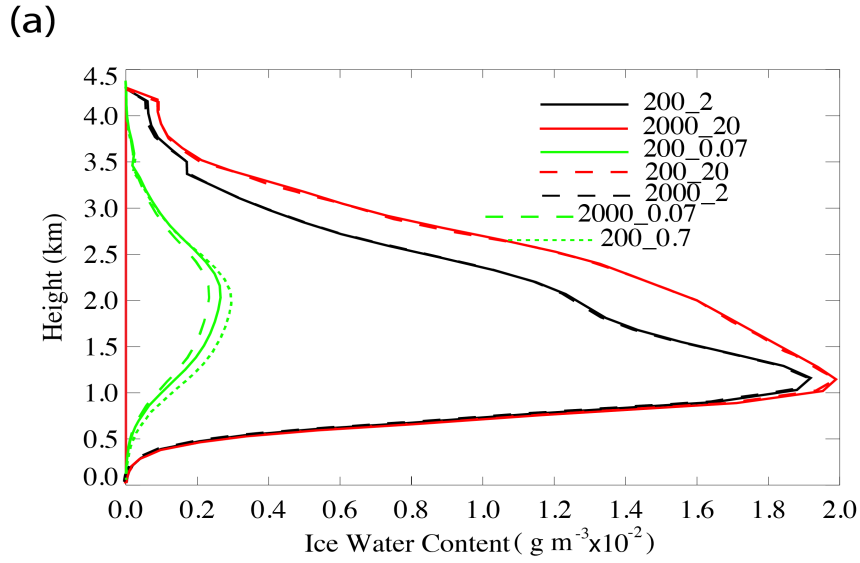
**Figure 7**



1937  
1938  
1939  
1940  
1941  
1942  
1943  
1944  
1945

Figure 8

Deleted: 6



Deleted:

Deleted:

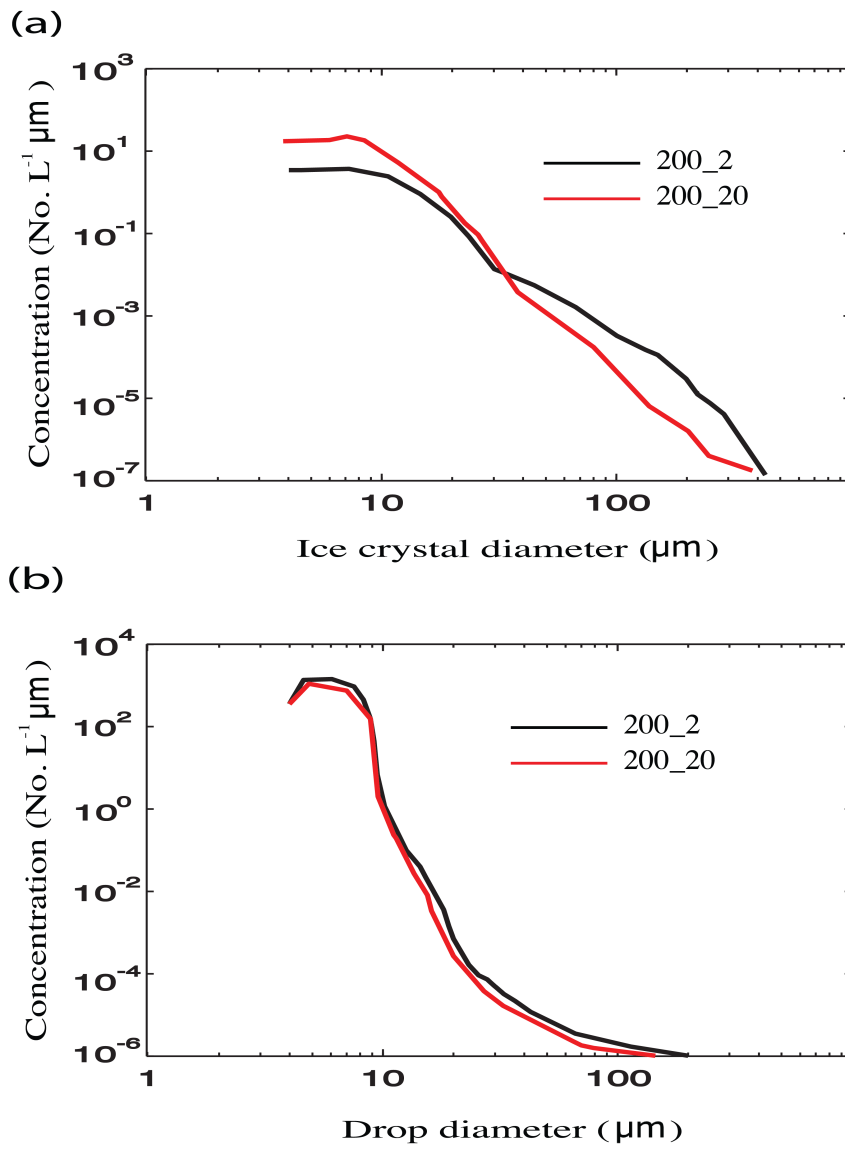
Deleted: 7

Figure 2

1948

1949





1953

1954

**Figure 10**

